FINAL
TECHNICAL SUMMARY REPORT
OF
RESEARCH AND DEVELOPMENT PROGRAM
OF
THERMIONIC CONVERSION OF HEAT TO ELECTRICITY

Volume II

July 1968

Contract Number NObs-90496
Project Serial Number SR-007-12-01
Order Number ARPA 219, Task No. 1 and Task No. 2
Program Code Number 3980

General Electric Company
NUCLEAR THERMIONIC POWER OPERATION
P. O. Box 846
Pleasanton, California

GEST-2062

FINAL
TECHNICAL SUMMARY REPORT
OF
RESEARCH AND DEVELOPMENT PROGRAM
OF
THERMIONIC CONVERSION OF HEAT TO ELECTRICITY

Volume II

July 1968

This work was supported by ARPA funds
through United States Navy, Bureau of Ships
Contract Number NObs-90496

Project Serial Number SR-007-12-01
Order Number ARPA 219, Task No. 1 and Task No. 2
Program Code Number 3980

General Electric Company
NUCLEAR THERMIONIC POWER OPERATION
P. O. Box 846
Pleasanton, California

LEGAL NOTICE

TABLE OF CONTENTS

LIST OF ILLUSTRATIONS

LIST OF ILLUSTRATIONS
(continued)

LIST OF ILLUSTRATIONS
(continued)

LIST OF TABLES

I. INTRODUCTION

This is Volume II of the second semi-annual and final technical summary report describing progress of the research and development program on thermionic conversion of heat to electricity under the Department of the Navy, Bureau of Ships Contract NObs-90496. The work performed under this contract is based upon and is a continuation of work initiated under contract NObs-88578. Both contracts were issued by the U.S. Navy, Bureau of Ships, and supported by the Advanced Research Projects Agency.

The objective of this program is the development of a nuclear thermionic electrical generating system for the Department of the Navy. Work under this contract is being performed to develop the material capabilities which are essential for this nuclear thermionic system. This work consists of three major tasks. Only the work accomplished on Task C is included in this volume. The statement of work to be accomplished under Tasks A and B is presented in Volume I.

Task C - Ceramic-to-Metal Seal Development
This task includes:

EFFORTS IN THE FOLLOWING AREAS ART OF PRESENT

(1) The development of cesium-resistant metallizing coatings for pure alumina ceramics;

(2) The development of molybdenum-alumina cermet structures for use as emitter-collector seal insulators.

(3) The evaluation and/or development of methods of bonding the metallic surface of insulators to structural metal numbers.

(4) Long-time testing of materials and seals at high temperatures in both vacuum and cesium vapor environments.

The over-all project responsibility for contract NObs-90496 at the General Electric Company is held by Dr. John E. VanHoomissen. The technical contributors with primary responsibility for the individual tasks are:

TASK A-1 - A. I. Kaznoff, Nucleonics Laboratory

TASK A-2 - R. A. Ekvall, A. I. Kaznoff, L. N. Grossman, Nucleonics Laboratory

TASK B - L. N. Grossman and A. I. Kaznoff, Nucleonics Laboratory

TASK C - R. H. Bristow, Tube Department

II. SUMMARY

Cesium resistant metallizing coatings for pure, polycrystalline, alumina ceramics were developed and evaluated by testing at 1250 and 1500°C in cesium vapor and vacuum environments. Molybdenum and tungsten based metallizing coatings containing small additions of refractory such as MgO, BaO, CaO, Y_2O_3, Al_2O_3, and mixtures of these oxides were investigated. Two grades of alumina were used in the investigation; a ultra high purity alumina Lucalox and a high purity (approximately 0.1 w/o silica) A-976 alumina. Based on vacuum tightness, peal strength, and microstructural appearances most of the coatings applied to A-976 alumina were acceptable whereas only several coatings were found acceptable for the Lucalox. In testing these coatings in vacuum and 20-torr cesium vapor for 850 hours at 1250°C, no changes in structure were detected. At 1500°C after 250 hours in vacuum, the coatings were still structurally stable. However, some structural changes were observed after testing for 230 hours at 1500°C in cesium vapor environment.

Graded cermets of molybdenum-alumina in which the structure was graded uniformly from an alumina to a molybdenum were developed and evaluated. The molybdenum-alumina cermets were fabricated with densities in excess of 98% theoretical density with good mechanical strength and vacuum tightness. Small additions (1 w/o) of yttria to the molybdenum-alumina cermets enhanced sintering and significantly improved the mechanical strength of the sintered bodies. The cermet bodies become electrically conducting where the molybdenum content is greater than 17 v/o. Techniques for fabricating multilayered hollow cermet cylinders

were developed. These multilayered cermet cylinders of various composition gradients remained vacuum tight after nine thermal cycles to 900°C followed by 327 hours at 1250°C.

Metal-to-metal joining of unalloyed molybdenum and tungsten to themselves, in combination, and to unalloyed niobium or tantalum were developed for joining metallized ceramics or cermets to the structural metal members of the seals. For this phase of the development program, tungsten-metallized ceramics were used because of their superior strength. Braze-diffusion-bonding, flow-type brazing and electron beam welding techniques of joining were investigated. Nickel was selected for braze-diffusion-bonding and the metals selected for flow-type brazing were chronium, iron, nickel, niobium, and palladium. Electron beam welding of molybdenum to a 25 v/o alumina-molybdenum cermet was successful however, the molybdenum cracked in the weld region. This cracking was believed to be caused by the resultant thermal stresses in the recrystallized molybdenum. Nickel braze-diffusion-bonding provided excellent bonds between niobium and molybdenum, tantalum and molybdenum, molybdenum and molybdenum, molybdenum and tungsten, and tungsten and tungsten. Excellent bonds between molybdenum and molybdenum, molybdenum and tungsten, and tungsten and tungsten were obtained by flow brazing with brazes of following compositions: 38 Cr-62 w/o Pd, 50 Nb-30 Pd-20 w/o Ni, and 67 Nb-33 w/o Fe. The 67 Nb-33 w/o Fe braze composition resulted in excellent bonding between niobium and molybdenum and tantalum and molybdenum.

High temperature (to 1500°C) tests were performed on metal-to-metal, metal-to-ceramic, and metal and ceramics in cesium vapor and vacuum environment to determine the resistant to cesium vapor and high temperature life capabilities. Nickel braze diffusion bond have a useful service temperature approaching 1500°C for the following material combinations:

1. Niobium-to-molybdenum or molybdenum-based metalized coating
2. Tantalum-to-molybdenum or to molybdenum or tungsten based metallized coatings.
3. Molybdenum-to-molybdenum based metallized coating.
4. Tungsten-to-tungsten based metallized coating.
5. Molybdenum-to-molybdenum-alumina cermets.

The 67 Nb-33 w/o Fe flow braze has a useful service temperature approaching 1500°C for the following materials:

1. Niobium-to-unmetallized alumina and to tungsten based metallized coatings.
2. Niobium-to-tantalum and molybdenum-to-molybdenum.
3. Tantalum-and molybdenum-to-tungsten based metallized coatings.

Bonds between molybdenum or tungsten and tungsten based metallizing produced by flow braze compositions 38 Cr-62 w/o Pd and 50 Nb-30 Pd-20 w/o Ni have a useful service temperature in range

of 1200 to 1500°C. The materials niobium, tantalum, molybdenum, and tungsten are compatible with cesium vapor up to at least 1500°C.

III. TECHNICAL PROGRESS

TASK C - Ceramic-to-Metal Seal Development

Introduction

Ceramic-to-metal seals that will have useful lives of many thousands of hours in a high-temperature, alkali-metal vapor atmosphere are needed for application as emitter-collector seal insulators in several designs of nuclear thermionic converters. The present effort seeks to further develop and test the several very promising sealing systems which were initially investigated under Contract NObs-88578.

The deficiencies of prior-art seals have been discussed in detail in a previous report.[1] These seals have been found lacking in two major characteristics; (1) chemical stability in the presence of high-temperature cesium vapor, and (2) thermal stability and/or compatibility of the component materials. Thus, efforts to provide the thermionic converter design engineer with useful sealing systems have centered around identification of materials possessing the required thermal and chemical stability and methods for joining them without introducing instability. The following sub-tasks comprised this effort:

C-1 - Cesium-Resistant Metallizing

C-2 - Graded Cermets

C-3 - Metal-to-Metal Joining

C-4 - Cesium and Vacuum Life Testing

---

* References appear on page 103

Sub-task C-1 - Cesium-Resistant Metallizing

Introduction

This sub-task comprised further development and evaluation of the cesium-resistant metallizing coatings for pure, polycrystalline alumina ceramics which were initially investigated under Contract NObs-88578.

The objective was the development of a material and method for applying a strongly adherent, metallic coating to the surface of a pure alumina ceramic, to which metallic members could be subsequently joined. The desired metallizing coating would be stable and resistant to cesium-vapor attack at temperatures up to 1500°C, would have a low sublimation rate, be pore-free, and would exhibit similar adhesive and cohesive strengths.

Results and Discussion

a. Effect of composition and temperature

The refractory-metal metallizing coatings which have been investigated contain small additions of refractory oxides to promote bonding to the alumina ceramic substrate. In most of these coatings, a liquid phase is formed which fills the interstices in the sintered metal layer and then solidifies (during cooling or through continued reaction with the alumina at the sintering temperature) to form a high-temperature-stable, solid phase. Oxides which have been investigated include MgO, BaO, CaO, Y_2O_3, Al_2O_3 and mixtures of these materials. Most effort, however,

has centered around the last three oxides.

Significant differences in structure of sintered coatings have been found to result from relatively small changes in composition (and thus melting behavior) of the oxide additions, from differences in the sinterability of the metallic phase and, as has been recently determined, by trace impurities in the alumina ceramic.

The first coatings which were studied were molybdenum-based and contained oxides which formed a ternary $MgO\text{-}CaO\text{-}Al_2O_3$ eutectic liquid at the sintering temperature. The ternary eutectic was initially chosen to provide a liquid phase at a low temperature (1345°C) in order to enhance -- at least not impede -- densification of the molybdenum coating. Later, it was determined that coatings containing binary mixtures of CaO and Al_2O_3 possessed structures and properties very similar to coatings containing ternary oxide compositions. Furthermore, it was found that at the sintering temperature, which was required to form the desired oxide phase at the interface, extensive densification of the molybdenum coating occurred, regardless of whether a binary or ternary oxide composition was used.

Adherence tests of such coatings, as well as occasional failure at the metallizing-ceramic interface after high-

temperature testing, indicated that less than optimum bonding was obtained with coatings in which the metallic phase sintered so dense that mechanical interlocking of the oxide phase with the metal phase was reduced. Although chemical bonding may play a role in achieving vacuum-tight structures, mechanical bonding is believed to contribute a major portion of the adhesive strength of a metallizing coating.

Several methods for controlling the density of the sintered metallic layer were then investigated, including the use of tungsten instead of molybdenum to reduce the sintering rate, and control of the melting behavior of the bonding oxide addition through chemical composition and precalcination.

Figure 1 shows the effect of sintering temperature on the structure of a molybdenum-based metallizing coating (No. 36 of Table 1) which contained an uncalcined bonding oxide composition corresponding to the calcium dialuminate - calcium hexaluminate (CA_2-CA_6) eutectic (80 w/o Al_2O_3, 20 w/o CaO). The equilibrium diagram for this system indicates that, at a metallizing temperature between 1720°C and 1850°C, CA_6 should exist in equilibrium with a liquid (transitory) and, upon cooling, CA_2 would crystallize out of the melt. The proportions of CA_2 and CA_6 in the interface layer at room temperature would be a function of the reaction temperature and the length of time it is

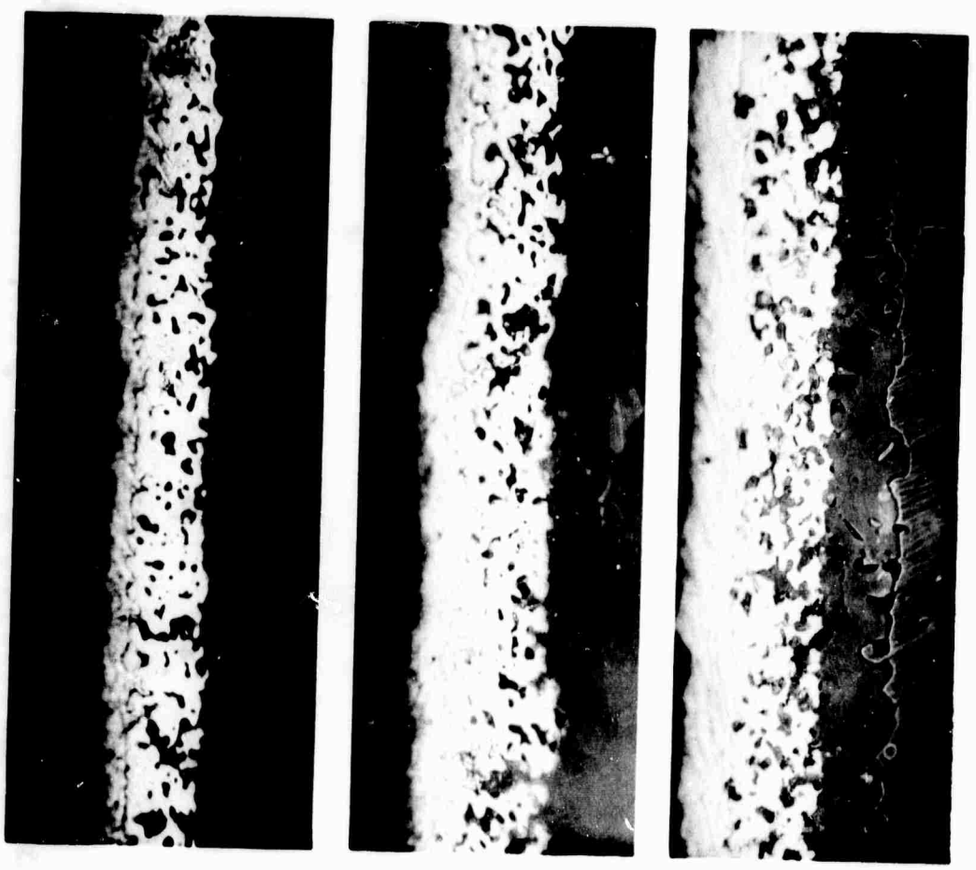

FIGURE 1 Effect of Sintering Temperature on Coating No. 36

TABLE I

Metallizing Compositions (Weight Percent)

Composition No.	Molybdenum M&R, Type P	Tungsten 5 u	Tungsten 2 u	Alumina Linde A	Alumina A-14 -325 Mesh	Calcium Carbonate	Yttrium Oxide	Calcine No. 114	Calcine No. 117
36	80.0			13.8		6.2			
60		98.0					2.0		
73		94.2			4.0	1.8			
114					85.9	14.1			
115		95.2						4.8	
117					50.6	49.4			
118		95.2							4.8
154			94.3		4.0	1.8			
155			95.2					4.8	
163			98.1			1.9			
169			95.1	4.9					
175			95.8		4.1	0.1			
176			95.2		4.7		0.1		
190			100.0						
191	100.0								
192			97.9		2.05	0.05			
193			97.6		2.35		0.05		
194	33.9		63.33		2.7	0.07			
195	33.9		62.93		3.1		0.07		

NOTE: All calcines heated 2 hours at 1200°C, plus 2 hours at 1400°C

held at this temperature. In the coating of Figure 1 - C, a relatively thick second phase layer exists at the interface. Only isolated patches of this phase are found at the interface of the coating after sintering at a slightly higher temperature, Figure 1-B. In Figure 1-A, no distinct interfacial phase layer exists, but a phase which is microscopically different from corundum appears in the interstices of the sintered metal layer.

X-ray diffraction analyses were made of the interface region between several different types of metallizing coatings on alumina; the coatings had been sintered at two temperatures -- 1835°C and 1875°C. Since the molybdenum or tungsten coating was too thick to be penetrated by the x-ray beam and the substrate was a thick alumina disc, the specimens were prepared by etching away the metal surface to expose the interface compounds. Table 2 summarizes the results obtained. Components are listed in order of their estimated abundance as they appear in the diffraction pattern.

Coating No. 36 was found to contain a large amount of CA_6 in the interface region of the specimen that was sintered at 1835°C, while only a trace of CA_6 was found after sintering to 1875°C. No CA_2 was detected in either coating. Although it has been previously postulated[2] that the interfacial phase layer of Figure 1 -C should contain a large proportion of CA_2, the

TABLE 2
X-Ray Diffraction Analyses

Metallizing Composition	Heat Treatment: 1200°C - 120 min, plus 1400°C - 120 min	Heat Treatment: 1835°C - 60 min	Heat Treatment: 1875°C - 60 min
No. 36		$CaO \cdot 6Al_2O_3$ Mo Al_2O_3	Mo Al_2O_3 $CaO \cdot 6Al_2O_3$
No. 60		W $3Y_2O_3 \cdot 5Al_2O_3$ Al_2O_3	W $3Y_2O_3 \cdot 5Al_2O_3$ Al_2O_3
No. 154		W $CaO \cdot 6Al_2O_3$ Al_2O_3	W Al_2O_3 $CaO \cdot 6Al_2O_3$
No. 114*	Al_2O_3 $CaO \cdot 2Al_2O_3$		
No. 117*	Al_2O_3 $CaO \cdot Al_2O_3$ poss. $CaO \cdot 2Al_2O_3$		
No. 117 on alumina		$CaO \cdot 6Al_2O_3$ Al_2O_3	Al_2O_3 $CaO \cdot 2Al_2O_3$

*Compositions 114 and 117 were calcined powders; all other samples were fused onto alumina substrates

x-ray data shows that this is not the case, at least not at 1835°C. CA_2 probably does exist in coatings sintered in the lower part of the 1720°C to 1850°C range (CA_2 was previously found by x-ray to be predominant in coatings sintered at 1750°C) and is responsible for the observed interfacial phase cracking (Figure 1-C) and consistent failure to obtain vacuum-tight seals with such coatings. The equilibrium diagram for the system indicates that, at a metallizing temperature between 1720°C 1850°C, CA_6 could exist in equilibrium with a liquid, and, upon cooling, CA_2 would crystallize out of the melt. It appears, however, that in the presence of the "infinite" supply of alumina (the substrate), reaction is sufficiently rapid that the melt disappears by reaction with alumina to form CA_6. Although the same amount of melt would initially be formed in the coating that was sintered at 1840°C (Figure 1-B), considerably less second phase (CA_6) is visible at the interface. This may result from flow of the superheated melt out of the coating onto the surrounding ceramic surface before it can react to form CA_6, by diffusion onto the alumina, or by volatilization of CaO. In the coating of Figure 1-A, sintered 20°C above the CA_6 melting temperature (1850°C), no second phase can be seen at the interface, although the oxide on the interstices of the coating appears different from the substrate. Furthermore, x-ray diffraction showed only a trace of CA_6. At this temperature, the liquid should exist in equilibrium with Al_2O_3 and, upon cooling, should

crystallize to Al_2O_3 and CA_6. Since the amount of CaO present in the coating is capable of forming a sizable quantity of melt (more than is formed at the CA_2-CA_6 eutectic), but since little CA_6 is found at the interface, loss of CaO must be occurring.

It will be noted that the interface between the metal phase and the substrate is rough -- the alumina has been eroded by the melts which form -- and the alumina appears to be growing out into and interlocking with the sintered metal "sponge". This interpenetration is believed to be the mechanism by which such coatings develop adherence. If the metal phase becomes too dense, the number of "fingers" of alumina interpenetrating the coating is reduced and the strength of adhesion decreases. Since the tensile strength of recrystallized molybdenum or tungsten is two to three times that of alumina, it would appear that maximum adhesion should be obtained when the coating at the interface contains approximately 2/3 alumina (by volume) and 1/3 metal. This structure, however, is difficult to achieve and it would probably be difficult to make a braze to it.

Figure 2 shows sections through specimens which had been metallized with a tungsten-based coating (No. 73) containing 25 v/o of an uncalcined oxide mixture having the 80 w/o Al_2O_3, 20 w/o CaO composition of the binary eutectic. This is the same oxide composition used in the molybdenum-based coating (No. 36) in Figure 1.

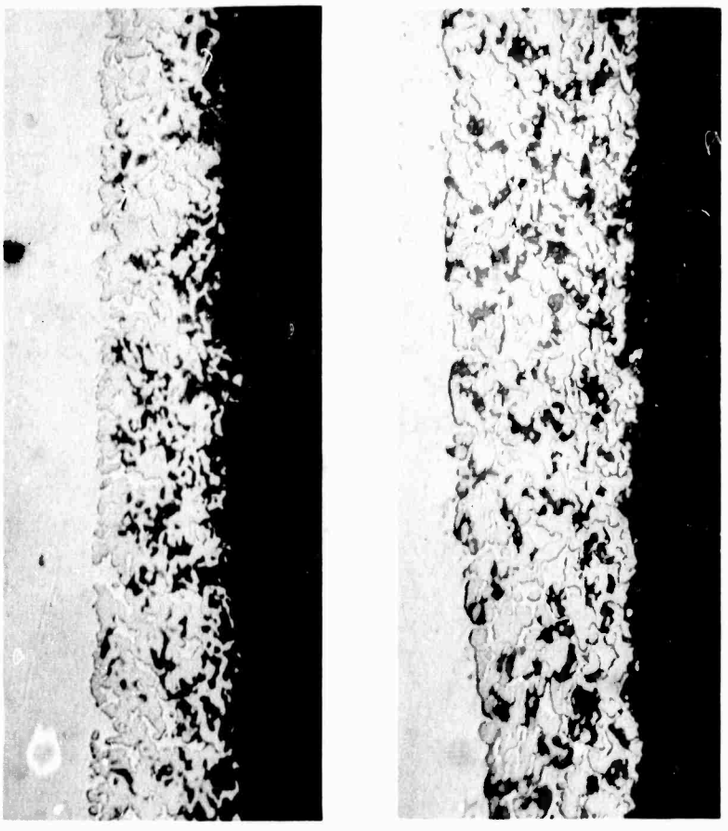

A
1870°C

B
1805°C

FIGURE 2 Effect of Sintering Temperature on Coating No. 73

The specimen in Figure 2-A was heated for one hour at a temperature of 1870°C, while the specimen of Figure 2-B was heated for one hour at 1805°C. In the former case, no interfacial phase layer is visible, while the expected layer is found in the latter specimen. Although the tungsten in Figure 2-A is adequately densified, providing near-optimum mechanical interlocking of the coating to the substrate, some unfilled pores and large voids exist near the midpoint of the coating. Near the interface, the pores are filled with oxide, while near the surface the pores are filled with braze alloy.

Unfilled pores probably exist in this coating because: (1) the pore size in the sintered tungsten layer is quite large (the tungsten was 5-micron average); (2) the melt which is formed within the coating, being of 1750°C eutectic composition, would be expected to flow to the interface or out of the coating where it could react with alumina to form a stable phase, CA_6; and (3) the coating only contained approximately 25 volume per cent of oxide.

Figure 3 shows the structure of coating No. 115, a 5-micron tungsten coating containing a prereacted bonding oxide composition (No. 114, Table 1) corresponding to calcium hexaluminate, CA_6. Although x-ray diffraction analysis (Table 2) showed only CA_2 and Al_2O_3 in the calcined powder (calcined 2 hours at

1400°C), CA_6 must form rapidly during heating to the metallizing temperature since a pressed pellet of the powder sintered, but did not melt, at a temperature just below the melting point of CA_6.

Thus, if a bonding oxide composition corresponding to CA_6 were used, no significant amount of liquid would form until a temperature of 1850°C was reached, the incongruent melting temperature of CA_6. At this temperature, the melt which is formed (approximately 70 w/o) would exist in equilibrium with alumina crystals (approximately 30 w/o) in the coating. A reduced tendency to flow out of the coating would be expected. Coating 115 of Figure 3 , shows a large volume fraction of oxide in the sintered coating.

Coating No. 155 of Figure 4 was similar to 115 but contained 2-micron tungsten. It can be seen to be well densified, with the interstices completely filled with an oxide phase. Vacuum-tight brazes were easily and reliably made to such coatings and peel testing of a strip of nickel, which had been gold-copper brazed to the surface of the coating, showed excellent adherence. Fracture occurred predominately through the alumina ceramic but partly through the coating, suggesting approximately equal cohesive and adhesive strengths. The use of 2-micron tungsten appears to provide a coating having the desired sinterability, a pore size which retains the oxide melt, and a sintered structure which

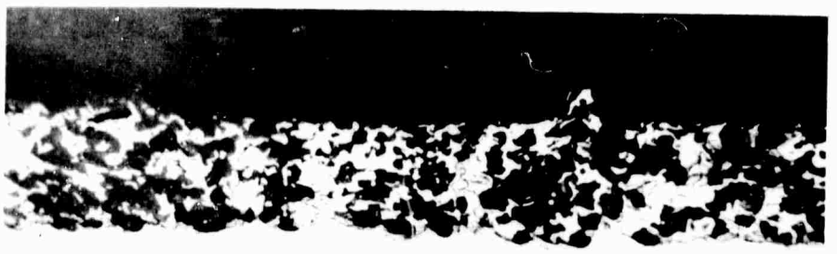

FIGURE 3 Coating No. 115 Sintered at 1870°C (500X)

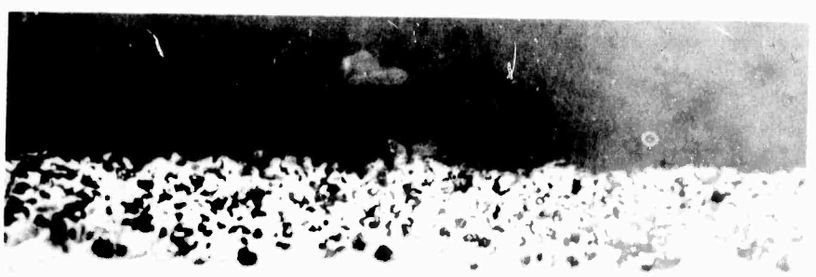

FIGURE 4 Coating No. 155 Sintered at 1870°C (500X)

provides nearly optimum mechanical interlocking with the substrate.

b. Effect of impurities on metallizing structure

At this point, it was observed that marked differences in structure occurred when many of the previously discussed coatings were sintered onto two polycrystalline alumina ceramics of near theoretical density but having different impurity levels. Figures 5 through 12 show the structure of many of the coatings of Table 1, when applied to these two alumina ceramics and sintered for one hour at 1870°C. One ceramic was General Electric's Lucalox* alumina, a polycrystalline alumina of near theoretical density prepared from an ultrapure grade of alpha alumina. The other ceramic was a composition designated A-976, a polycrystalline alumina of near theoretical density but prepared from a Bayer process alumina containing a fraction of one per cent total impurities. Silica analyses of these compositions were attempted but proved inconclusive. Unfortunately, the unreliability of the silica analyses was not determined until near the end of the program. Several different specimens of A-976 analyzed to contain between 0.05 and 0.11 w/o silica. The very pure Lucalox, on the other hand analyzed to contain 0.08 w/o silica. Although some silica may have been picked up during processing, an increase of this magnitude over the few

*General Electric trade mark for a high-purity alumina ceramic

parts per million present in the raw alumina seems unlikely. The raw material from which body A-976 is prepared contains less than 0.2 w/o total, Na_2O, SiO_2, and Fe_2O_3. A fractional percentage of MgO is purposefully added as a grain growth inhibitor. Microscopic examination of A-976 often shows small isolated pockets of a second, apparently glassy, phase at grain boundaries. X-ray microprobe analysis has shown this phase to contain silicon. No such particles have been seen in Lucalox alumina.

Thus, it appears that the small amount of impurities in A-976 influence the structure of a metallizing coating -- probably through their effect on the viscosity of the liquid phase which is formed at the sintering temperature. This effect will now be examined for coatings with and without oxide additions.

Figure 5 shows the structure of a pure 2-micron tungsten coating sintered onto body A-976 as well as the same coating on Lucalox. Both are completely permeated by the gold-copper braze (each specimen was brazed to a nickel strip with a 35-per cent gold - 65-per cent copper alloy for peel testing) and show negligible bonding to the ceramic. This is the structure which would be expected, since no reaction occurs between pure tungsten and aluminum oxide at this temperature. The scattered particles of oxide in the coating on Lucalox probably results from impurities in the tungsten as well

as alumina particles derived from ball milling in a pure alumina mill. A slightly higher level of oxide content is seen in the coating on A-976.

Figure 6 shows a coating, No. 169, consisting of tungsten plus 20 v/o Linde A alumina. On both ceramics the coating is well sintered, but contains a few unfilled pores.

Coating No. 163, comprising tungsten with approximately 1 w/o calcium oxide (added as calcium carbonate) is shown in Figure 7. This is sufficient calcium oxide to form approximately 20 v/o melt by reaction with alumina upon heating to the sintering temperature. Since the reaction must occur at the interface, it might be expected that the interstices in the sintered tungsten coating would be unfilled by oxide. Such is the case on Lucalox, as shown in Figure 7. When sintered onto A-976, however, most of the interstices of the coating are filled with oxide and an excellent coating, showing good adhesion, results. This is probably due to the effect of the trace impurities in the ceramic upon the viscosity and crystallization characteristics of the melt.

Coating No. 60, Figure 8, is similar to coating No. 163 but contains Y_2O_3 instead of CaO. The 2 w/o Y_2O_3 would form approximately 19 v/o liquid at 1760°C through reaction with alumina at the interface. Again, the coating on Lucalox is completely permeated by braze and shows very poor adherence to the ceramic. On A-976, however, an excellent coating is obtained. Coatings

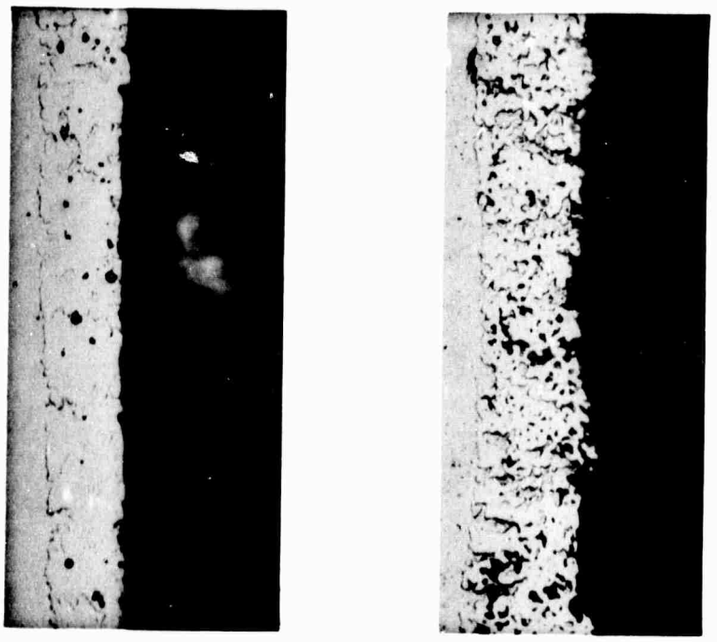

FIGURE 5 Coating No. 190 on Lucalox and A-976 Alumina (500X)

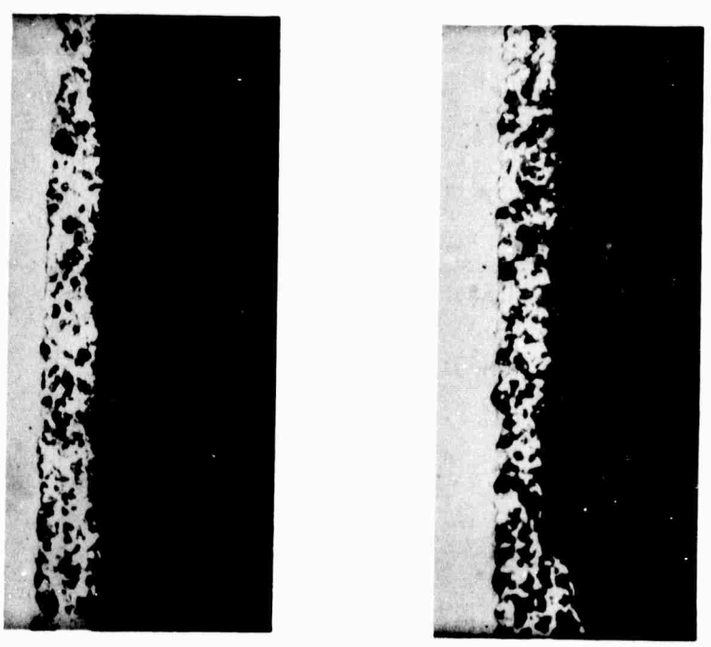

FIGURE 6 Coating No. 169 on Lucalox and A-976 Alumina (500X)

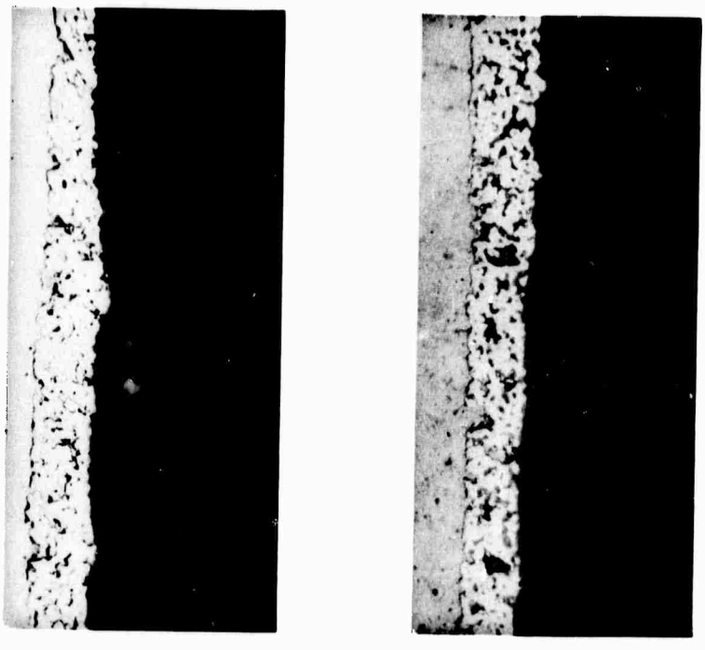

FIGURE 7 Coating No. 163 on Lucalox and A-976 Alumina (500X)

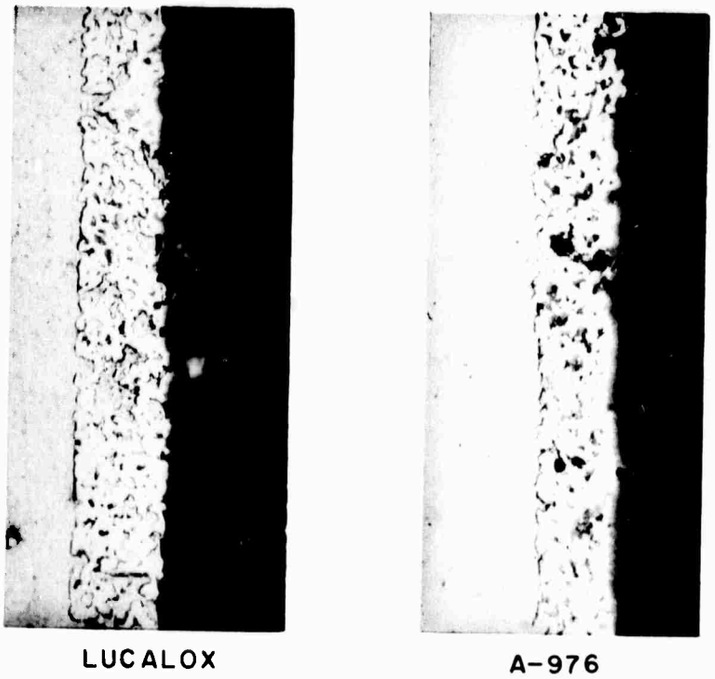

FIGURE 8 Coating No. 160 on Lucalox and A-976 Alumina (500X)

Nos. 154 and 155 on Lucalox and A-976 are shown in Figures 9 and 10.

Several coatings were prepared which contained tungsten and alumina (like No. 169), but with the further addition of a very small amount of either CaO or Y_2O_3. The objective was to form a thin film of liquid on the surface of the alumina particles in the coating during sintering, thereby aiding densification of the coating and bonding to the substrate, yet retaining an oxide phase within the coating. Whereas coating No. 169 formed no liquid phase, coating No. 155 (bonding oxide composition was CA_6) theoretically formed mostly liquid at 1850°C, and coating No. 163 (only CaO) formed a series of liquids at the interface during heating to the sintering temperature, these new coatings would form a small amount of each succeeding eutectic liquid on the surface of the alumina particles in the coating during heating, and the oxide additives would never be totally liquified.

Coating No. 175 contains approximately 20 v/o oxide and, at the sintering temperature the oxide additions (Al_2O_3 and CaO), theoretically would be approximately 20 per cent liquified. Coating No. 176 contains approximately the same total amount of oxide (Al_2O_3 plus Y_2O_3), but would be approximately 25-per cent liquid. The structures of these coatings after sintering one hour at 1870°C are shown in Figures 11 and 12.

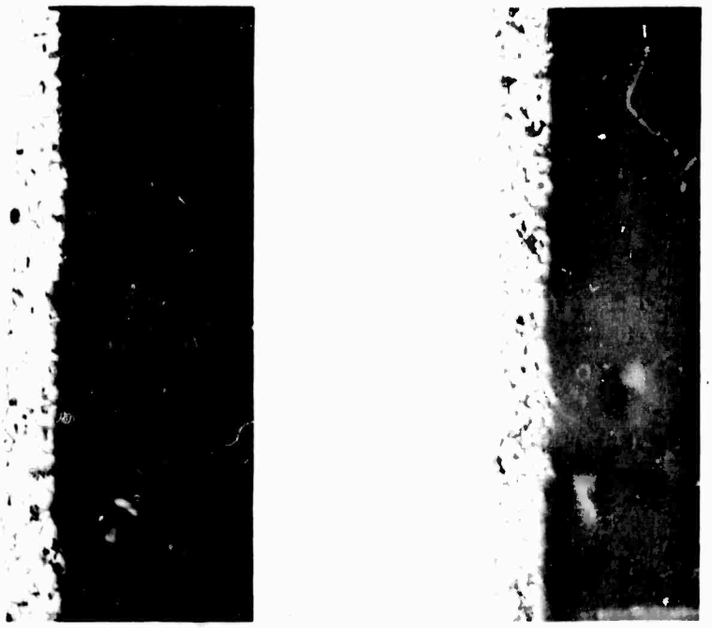

LUCALOX A-976

FIGURE 9 Coating No. 154 on Lucalox and A-976 Alumina (500X)

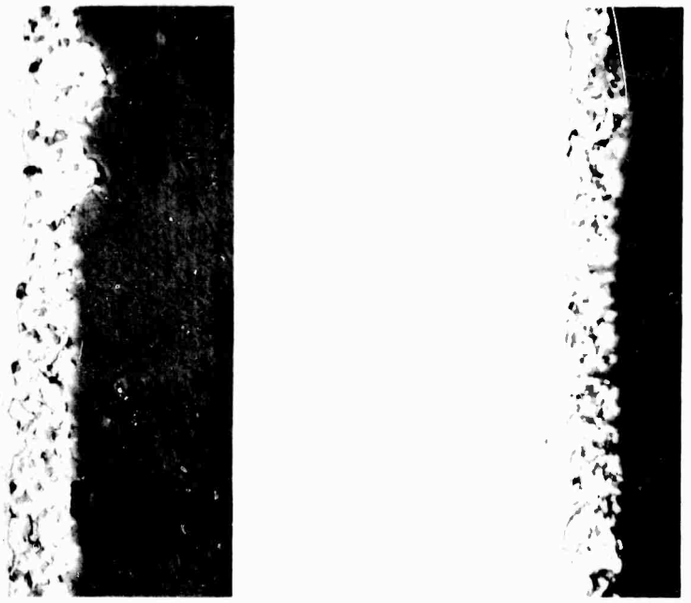

LUCALOX A-976

FIGURE 10 Coating No. 155 on Lucalox and A-976 Alumina (500X)

FIGURE 11 Coating No. 175 on Lucalox and A-976 Alumina (500X)

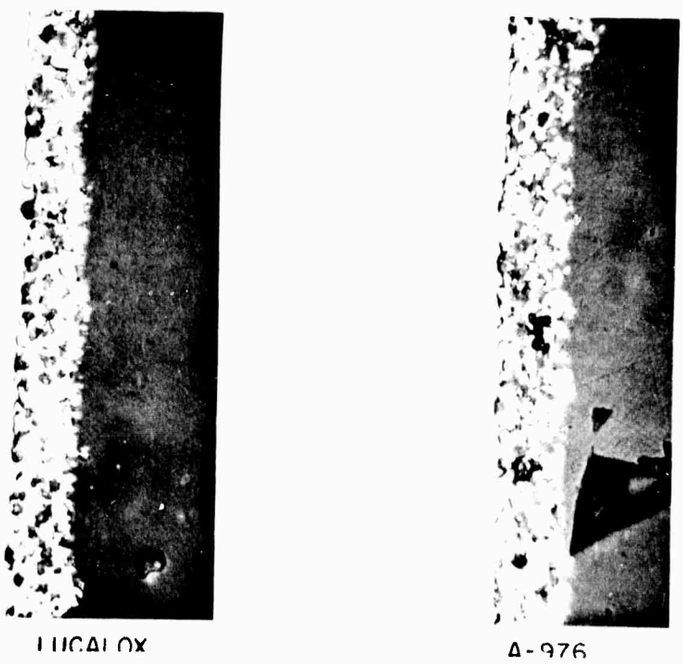

FIGURE 12 Coating No. 176 on Lucalox and A-976 Alumina (500X)

Compositions Nos. 192 and 193 were similar to Nos. 175 and 176, respectively, but the total oxide content was reduced approximately 50 per cent. Figure 13 shows the structure of coating No. 192.

Composition No. 194 was similar to No. 192, except that molybdenum had been substituted for part of the tungsten. The molybdenum content of each coating was approximately 35 w/o. The effect of molybdenum on sintering of the metallic phase is readily apparent by comparing Figures 14 and 13.

Although the photomicrographs adequately show the gross differences in structure which exist in these many coatings, careful microscopic examination, at several different magnifications, is required to distinguish the subtle differences in density, porosity, metal-oxide ratio, and permeation by braze alloy, which augment test data in selecting a preferred composition.

Gold-copper alloy is unsuited for use in high-temperature seals; however, it is eminently suited to the preparation of test specimens for the evaluation of vacuum tightness and mechanical strength, since the reliability of such brazes to conventional metallizing coatings is well established. Most test specimens consisted of rings (approximately 0.620 inch outside diameter, 0.420 inch inside diameter, 0.200 inch long) metallized on one face, and brazed to either side of a metal washer to form a

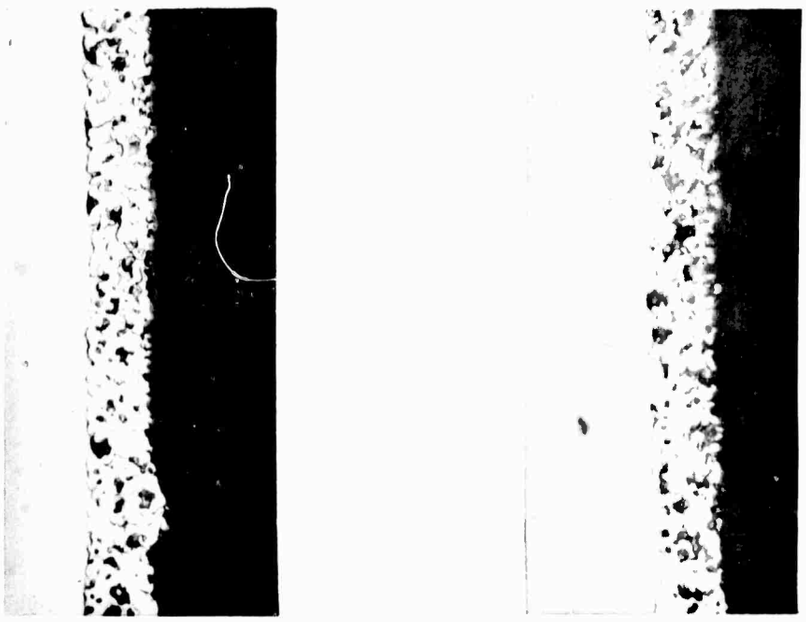

FIGURE 13 Coating No. 192 on Lucalox and A-976 Alumina (500X)

FIGURE 14 Coating No. 194 on Lucalox and A-976 Alumina (500X)

specimen for helium leak testing, thermal cycling, and high-temperature cesium corrosion and vacuum life testing. Gold-copper was, of course, never used in any seals subjected to high temperatures. A qualitative peel or adherence test was performed using a single metallized ring, gold-copper brazed to a strip of nickel. It was usually possible to correlate the appearance of the component parts after peel testing with the microstructure of the coating and interface region. For example, coatings in which the refractory metal sintered to an extremely dense layer stripped easily from the ceramic surface with only a few grains of ceramic adhering to them.

Based upon vacuum tightness, peel strength and microstructural appearance, most of the coatings which were applied to body A-976 were acceptable and several were excellent. Based upon the relatively few specimens of each type which were examined, the estimated order of preference would be coatings No. 175, 176, 169, 155, 192, 193, 60, 154. Fewer coatings were deemed acceptable when sintered onto Lucalox. Several, however, were quite satisfactory and yielded consistently reliable seals, including 175, 176 and 169.

c. Environmental testing

Testing of metallized alumina specimens, and seals prepared from them, was performed at temperatures of 1250°C and 1500°C in vacuum, as well as in 20-Torr

cesium vapor. Changes in microstructure of seals incorporating metallized ceramics are discussed in the section "Metal-to-Metal Joining". In this section, only the effect of temperature and environment on exposed (unbonded) metallized surfaces are considered.

Alumina rings metallized with several of the previously discussed coatings, were exposed for 855 hours at a temperature of 1250°C to two different environments -- vacuum (10^{-6} range) and 20-Torr cesium vapor. No changes were detected in any of the metallizing coatings by careful microscopic examination of polished sections after either type of treatment. Included were coatings such as No. 73, which contained a considerable amount of oxide, as well as coatings such as No. 60, which contained relatively little oxide.

When tested for 230 hours at 1500°C, however, changes were detected in several of the coatings which were exposed to cesium vapor, Figures 15 and 16. The specimens tested in cesium and in vacuum were brazed together after testing. In coatings which initially contained considerable oxide, such as No. 155 (similar to coating No. 73) the second phase in the coating became quite evident as a result of the formation of sharp line of demarcation between this phase and the alumina substrate as shown on the left in Figure 15-B. The specimen tested at 1500°C in vacuum, right side of Figure 15-B, showed no detectable change.

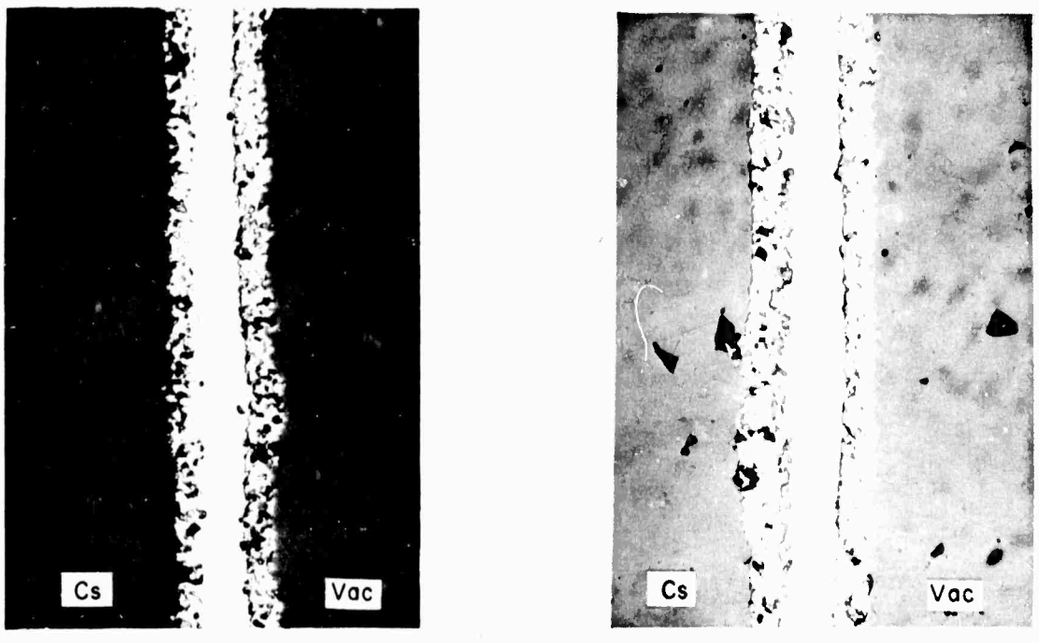

A
LUCALOX

B
A-976

FIGURE 15 Coating No. 155 on Lucalox and A-976 Alumina After 230 Hours at 1500°C (250X)

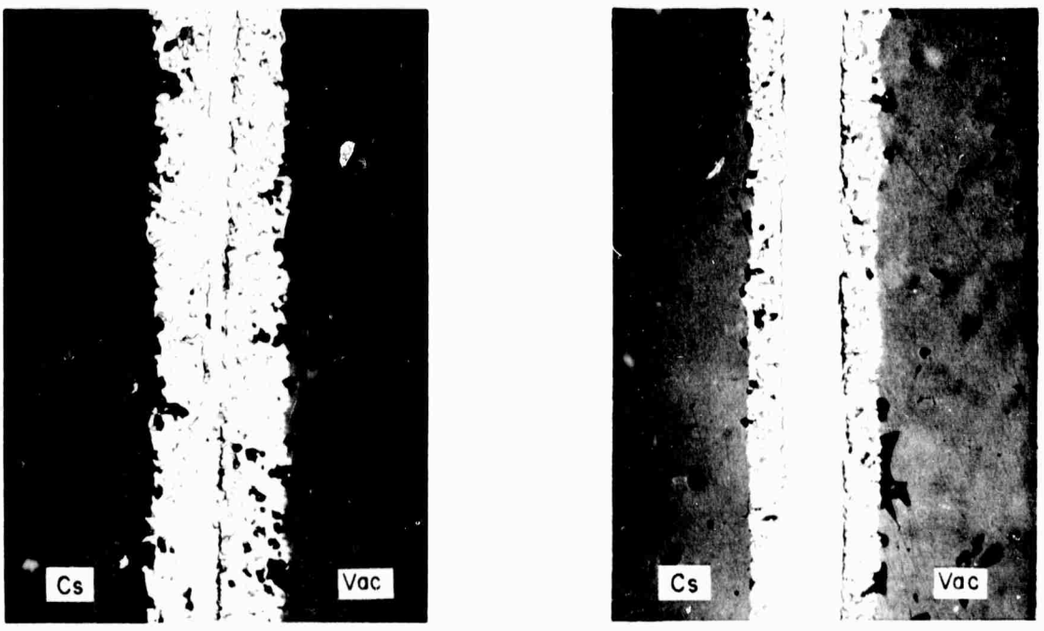

A
LUCALOX

B
A-976

FIGURE 16 Coating No. 60 on Lucalox and A-976 Alumina After 230 Hours at 1500°C (250X)

The same effect was also noted in coatings which initially contained less oxide, such as No. 60 in Figure 16, although it was less pronounced because of the lesser quantity of second phase initially present.

As mentioned previously, coating No. 60 on Lucalox (Figure 8), typically was very porous and became permeated by braze alloy. Any changes which occurred during cesium and vacuum testing were not detectable because of the poor quality of the initial coatings.

Coating No. 155 on Lucalox changed little upon heat treatment in vacuum, but changed noticeably as a result of testing in cesium. Although no second phase layer became evident, there occurred a coarsening (sintering) of the tungsten structure as shown in Figure 16-A.

It is believed that the observed changes in these two coatings resulted from reaction between the oxide phase in the coating and the cesium or cesium oxides in the test environment. It is significant to note that no such change occurred in seals which were tested in cesium, seals wherein the coating was not directly exposed to the cesium vapor environment.

Conclusions

1. Several molybdenum and tungsten-based metallizing coatings for pure alumina ceramics have been developed which possess the required high-temperature stability, vacuum tightness and mechanical strength.

2. Significant differences in the structure of coatings applied to two different alumina ceramics have been observed, and are believed to result from the effect of trace impurities (predominately silica) in the ceramic. The best coatings were associated with the ceramics of highest impurity level.

3. Coatings possessing the required strength and vacuum tightness, have been identified for use with the very pure Lucalox alumina.

4. No changes in structure were detected in coatings tested for as long as 850 hours at 1250°C in vacuum and in 20-Torr cesium vapor.

5. No changes in structure were detected in coatings tested for 230 hours at 1500°C in vacuum.

6. Changes in the appearance of the interfacial phase were noted for coatings tested at 1500°C in cesium vapor. It was not determined whether the observed changes were the effect of cesium or impurities in the cesium atmosphere.

Sub-task C-2 - Graded Cermets

Introduction

The purpose of this task was the further development and evaluation of graded, insulating, cermet structures which were initially demonstrated to be feasible under Contract NObs-88578. This approach comprises joining the metallic members of the device to the surfaces of a multilayered or graded cermet, the cermet consisting of an insulating oxide core with integrally

bonded metallic surface layers. The structure may grade smoothly in composition from a predominately oxide core to a predominately metallic surface layer, or it may occur in discrete layers. In either case, it is important (in systems where the metal and oxide possess different thermal expansion characteristics) to have a composition gradient that will minimize internal stresses.

The system molybdenum-alumina was chosen for the fabrication of cermets because of their known high-temperature compatibility and low vapor pressures. As will be discussed later, the large thermal expansion mismatch which exists between molybdenum and alumina sets up severe stresses and necessitates a carefully designed gradation in composition from insulating core to metallic surface. Tungsten was not considered because it is more difficult to sinter to a vacuum tight structure and its low thermal expansion would make gradation even more difficult. Although niobium and tantalum would provide a much improved expansion match (almost ideal in the case of niobium), the potentiality of their reaction at the test temperature of 1500°C, their rapid embrittlement by interstitials, and the need for sintering in an extremely pure vacuum or inert atmosphere relegated them to second choice. Recent data, however, indicates that negligible reaction occurs between niobium and alumina at 1500°C (this is in marked contrast with the tantalum-alumina system) making this system extremely attractive for further study.

Results and Discussion

a. Effect of composition on properties

For the preparation of graded or multilayered cermets from mixtures of molybdenum and alumina powders, it is desirable to use materials which undergo the same total shrinkage during sintering and, preferably, which densify at the same rate. Several closely matched systems of materials had been previously identified[1], including M & R Type P molybdenum with Alcoa A-14 (minus 325 mesh) alumina, and G-E 61-8-1 molybdenum with Linde A alumina. The large difference in total shrinkage exhibited by compositions within these two systems of materials results from their distinctly different particle size distributions.

In this section, sintering "shrinkage" is based upon the final (sintered) dimension of the specimen.

Thus, percent shrinkage = $\frac{\text{Pressed dia.} - \text{Sintered dia.}}{\text{Sintered dia.}}$

*Tables 3 through 10 contain data on the sintering behavior or molybdenum-alumina cermets as affected by composition, magnesia or yttria additions, organic binders, mixing technique, pressing pressure and sintering temperature.

It is desirable to use as high a molybdenum content as possible in the core layer of a metallized cermet in order to reduce its aggregate thermal expansion and, thus, reduce the expansion mismatch with the adjacent, slightly more metallic layers. Table 3 series E shows that electrical

---

*Tables 3 through 12 appear on pages 51 through 60
Densities in excess of theoretical occurred because of minor discrepancies in weighing the molybdenum and alumina.

conductivity will occur when the volume percentage of molybdenum is increased to some value between 15 and 20 v/o. Table 7 contains data for wet ball milled and, consequently, well homogenized blends of powders, and shows that conductivity occurs at a value somewhat greater than 17 v/o molybdenum. Graded cermet structures were subsequently prepared using both the 10 and 15 v/o molybdenum composition as the core layer and no conductivity was measured through any of these specimens provided the batch was wet milled to assure homogeneity.

Table 3 shows that, under the sintering conditions employed, densification of several types of alumina, as well as molybdenum-alumina cermets, is inhibited when the MgO content exceeds 0.25 w/o. Test series C and D show that the density of a 25 w/o molybdenum-alumina cermet more closely approaches theoretical density when the MgO is introduced as magnesium carbonate rather than magnesium hydroxide. In subsequent tests, Tables 7, 8, 9, 10, the MgO content was reduced to 0.12 w/o with equally high densities being obtained.

Figure 17 shows a section through one wall of a hollow, cylindrical, seven-layer graded cermet whose constituent layers had been prepared by wet mixing. This structure was electrically insulating (10 w/o molybdenum core) and vacuum tight in spite of the considerable inhomogeneity of composition. Figure 18, on the other

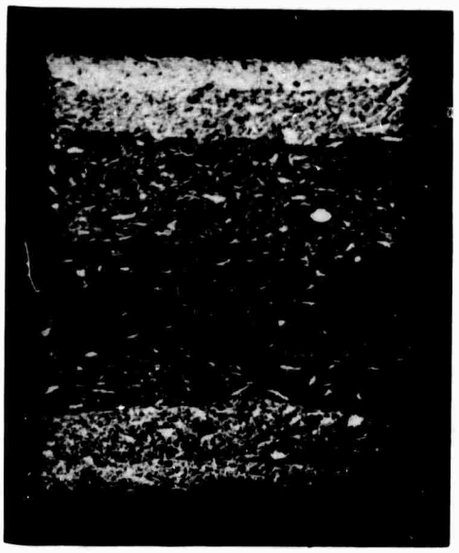

FIGURE 17 Section Through One Wall of a Seven-Layer Cermet Cylinder Showing Inhomogeneities (16X)

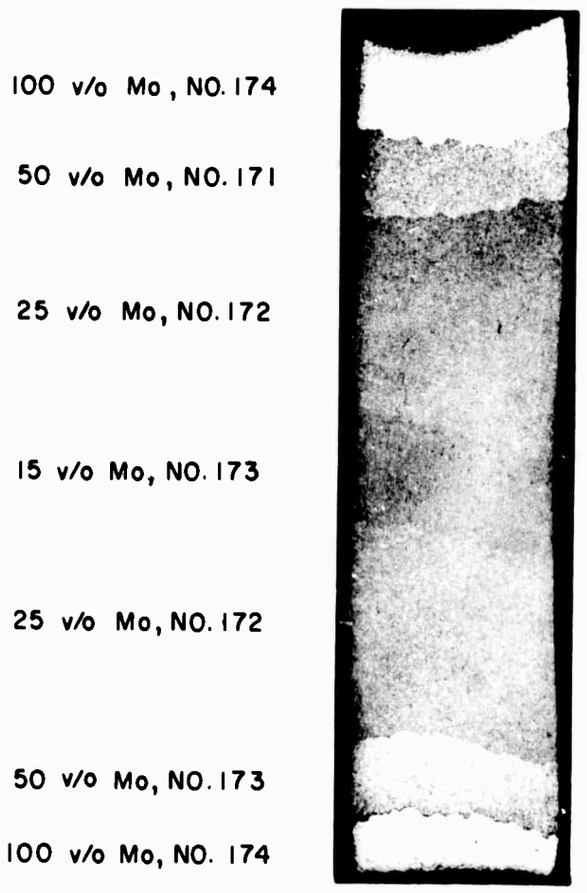

FIGURE 18 Section Through One Wall of a Cermey Cylinder Showing Desirable Homogeneity of Structure (9X)

hand, shows a section through a similar cermet, but whose constituent layers had been prepared by wet ball milling. Much better homogeneity is apparent. This particular structure consisted on an insulating 15-v/o molybdenum core (composition No. 173), with adjacent more metallic layers (No. 172, 25-v/o molybdenum; No. 171, 50-v/o molybdenum), and with pure molybdenum surface layers (No. 174). This structure was crack free and vacuum tight. The dark lines which appear at the interface between layers were caused by relief polishing.

Figure 19 shows the microstructure of each of these yttria-containing compositions at 250 X. The excellent homogeneity and nearly pore-free structures obtained is readily apparent. Many of the "pores" in Figures 19 and 20 are due to pull-out of alumina grains during polishing.

Figure 20 shows the structure of a series of molybdenum-alumina cermets whose molybdenum contents progressively decrease by approximately 13 v/o.

b. Yttria-containing cermets

Table 4 contains the results of a series of tests to determine the effect of small additions of yttria on the densification of alumina and molybdenum-alumina cermets. It was expected that densification would be promoted through the formation of a small amount of liquid phase at the sintering temperature.

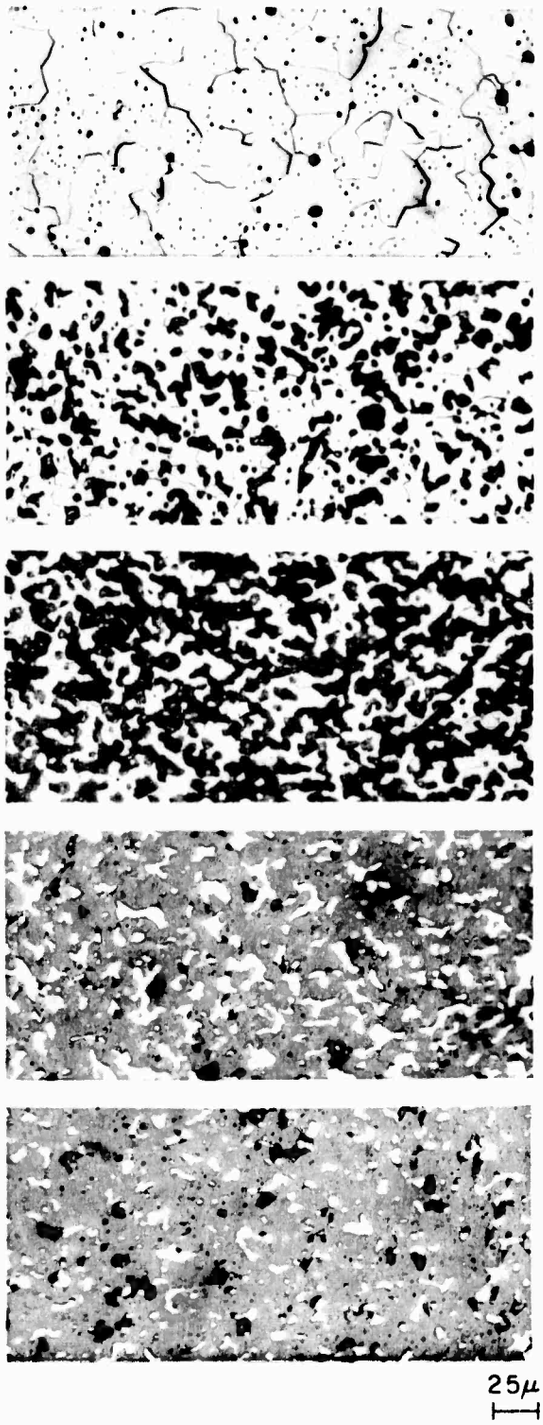

FIGURE 19 Microstructure of Molybdenum-Alumina Cermet Compositions Containing Yttria

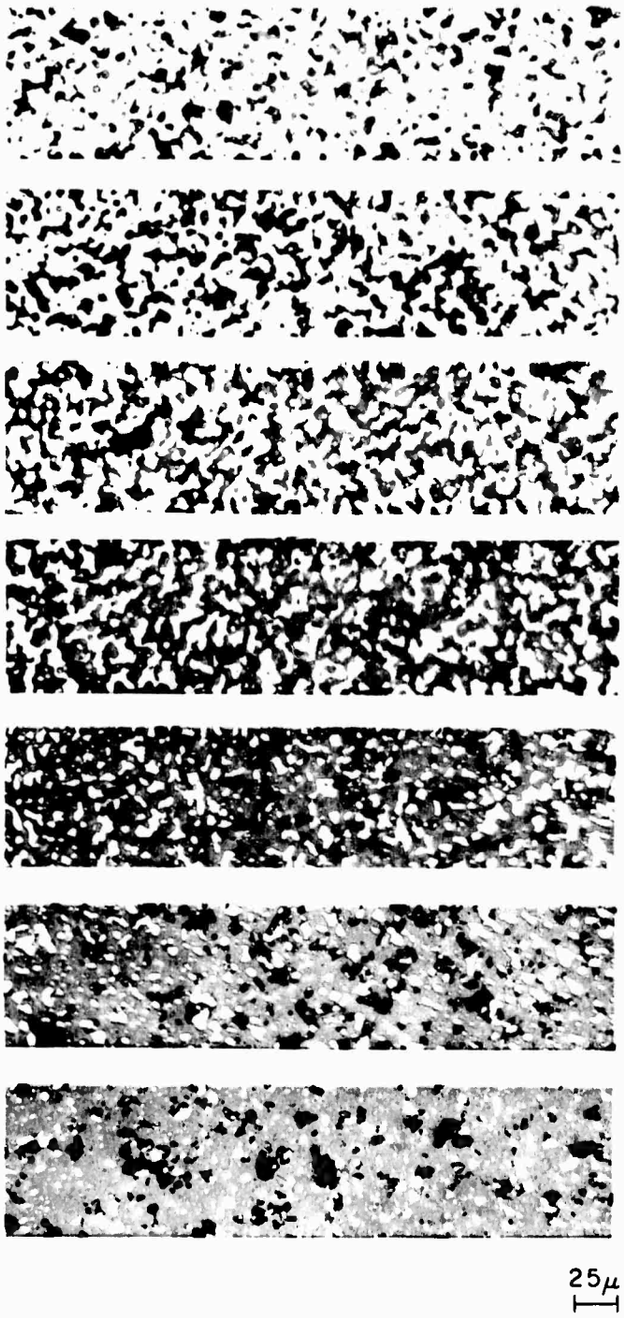

FIGURE 20 Microstructure of Molybdenum-Alumina Cermets

Test series A shows that at a temperature of 1800°C, the densification of alumina is improved with additions of yttria up to 4 w/o. At a temperature of 1900°C and above, however, the sintered density decreases when the yttria content is greater than 1 w/o.

With a 1 w/o addition of yttria, molybdenum-alumina cermets containing from 75 v/o to 15 v/o molybdenum sintered to densities in excess of 98 percent of theoretical at only 1800°C. The composition with the smallest volume fraction of metal, 15 v/o, attained a density of 99.5 percent of the theoretical value. It is interesting to note that at this same temperature a 1 w/o yttria-alumina specimen, with no molybdenum present, attained a density of only 95.2 percent.

Table 5 contains additional data for yttria-containing cermets which had been wet ball milled in xylene, dried, pressed at 20 tons per square inch, and sintered to 1900°C.

c. Effect of organic binders on densification

A temporary organic binder and/or lubricant is necessary in the compaction of most ceramic and metal powders in order to provide internal lubrication of the powder during pressing, to provide die-wall lubrication, to promote green strength, and to facilitate granulation of the powder. The densification behavior of several cermet compositions as well as their constituent powders, with various percentages of several organic binders, is given in Table 6.

During ejection of a compact from a polished tungsten-carbide die it was noted that specimens containing less than about 3 w/o binder chattered and squealed while those containing approximately twice as much binder ejected easily and inaudibly. It was also found that approximately 6 w/o binder, either cetyl alcohol or paraffin, was required in order to press multilayered cermet specimens free of laminations through or between layers. Although cetyl alcohol was found to be a satisfactory binder and die lubricant for molybdenum and A-14 alumina, it was far less effective than paraffin in the fine Linde A powder. Even with 7 w/o paraffin, however, compositions containing high percentages of Linde A (Nos. 184 and 185, Table 8) stuck badly to the punch faces.

The data of Table 6 indicate that the amount or type of binder, within the limits studied, has a small but significant effect on the shrinkage and density of cermet powders. The sintered density of alumina is little affected by high pressing pressures, while the density of molybdenum and molybdenum-alumina cermets is improved by higher pressing pressures. This is fortuitous since higher pressing pressures are generally advantageous in reducing the spread in shrinkage between metal-rich and oxide-rich compositions.

The relationship between sintering shrinkage and cermet composition is quite complex as shown by the data of Tables 5 through 10. The data of Table 6 series

C, shows that the shrinkage of cermets containing 25 and 50 v/o molybdenum is higher than that of cermet compositions which are either richer or poorer in molybdenum, or of molybdenum or alumina alone, when pressed at 20 tons per square inch. When pressed at only 10 tons per square inch, sintering shrinkage decreases continually as the composition is changed from 75 v/o to 10 v/o molybdenum.

Table 7 shows similar data for compositions containing a different lot of molybdenum powder (lot number 7213) and containing a different binder. Here there appears to be a progressive decrease in shrinkage as the volume fraction of molybdenum decreases, at both 10 and 20 tons per square inch.

Table 5 shows the same interrelationship of shrinkage, composition and pressure for yttria-doped compositions, but containing the same lot of molybdenum and the same type and amount of binder as used in the bodies of Table 7.

Table 10 contains data on compositions similar to those of Table 7, but containing one-half as much binder. When pressed at 10 tons per square inch, sintering shrinkage is a maximum near the 50 v/o molybdenum composition, as was the case in Table 6.

Cermets containing Linde A alumina, Table 8, showed higher shrinkages and a progressive decrease in shrinkage with decreasing molybdenum content.

Cermets containing a blend of A-14 and Linde A alumina powders, Table 9, showed a shrinkage minimum near 25 v/o molybdenum, in contrast with the shrinkage maximum found in Table 10.

Large differences in shrinkage and sintered density of different lots of the same brand and grade of molybdenum powder were also noted. Tables 3 and 7 show that lots 6856 and 7213 attain similar densities, but with different total shrinkages, while lot 7234 sinters to a much lower density, even at high pressing pressures.

d. Pressing of multilayered cermets

Initially, considerable difficulty was encountered in the preparation of multilayered molybdenum-alumina cermets which were vacuum tight and free from laminations after sintering. In many cases, specimens could be pressed (either in a cemented carbide die or isostatically) which were lamination-free but they would develop small laminations during sintering.

Two major contributors to lamination were found to be low green strength within or between layers, and differences in shrinkage rates and total shrinkage of the several layers during sintering. Increasing the temporary organic binder content to 7 w/o and the use of a material -- paraffin -- which served both as a binder and an internal lubricant, eliminated the formation of laminations from the first mentioned cause. A series of experiments revealed that inhomogeneity of composition and nonuniform pressing pressure were the two

biggest contributors to laminations during sintering. Homogeneity was improved significantly by ball milling the compositions in an organic solvent containing the binder in solution. Attainment of uniform pressing pressure (during double-action pressing of hollow cylinders in a cemented carbide die) was achieved through two means: (1) more uniform loading of the die cavity and (2) simulated axial isostatic pressing. Uniformity of loading of the die with each successive layer of powder was attained by vibratory feeding of screened granules to the die as it rotated slowly about its axis. The feeder consisted simply of a hopper with a small hole in one end, which was vibrated in the proper direction by a six-volt door buzzer. The powder was granulated by screening the dried cake through 45 onto 120 mesh. Other size fractions were used with equally good results.

Simulated isostatic pressing was achieved by inserting a rubber washer between the upper punch and the powder prior to pressing. The rubber washer was sliced from a cylinder of a relatively hard RTV silicone rubber which was cast in the same die as used for pressing the cermets. The effectiveness of the rubber washer was demonstrated by pressing, with and without the washer, powders which had been intentionally nonuniformly loaded into the die. Without the rubber washer, laminations were usually visible upon ejecting the piece from the die.

Although all of the above discussed corrective measures were necessary, the use of the rubber washer is believed to be the single, most important factor in achieving lamination-free multilayered cermet specimens.

Figures 21 and 22 are photographs of several graded cermet cylinders (approximately 5/8-inch outside diameter, 13/32-inch inside diameter). "Hourglassing" due to differential shrinkage between the ends and the midpoint of the cylinder is evident. In most of the cylinders shown, the central region experienced a higher shrinkage than the ends due to a lower pressed density which, in turn, resulted from loss of pressure caused by die wall friction. Thus, although the shrinkage of a test disc of 15 v/o molybdenum-alumina cermet is generally lower than that of a 75 v/o composition (when pressed at 20 tons per square inch), it undergoes a higher shrinkage when incorporated in a die-pressed graded cermet.

Another type of failure encountered in the preparation and testing of graded structures was radial cracking through the central layers due to differential contraction of these layers and the immediately adjacent layers upon cooling from a high temperature. The higher thermal contraction of the alumina-rich layers, as compared with the molybdenum-rich layers, caused a circumferential tension or hoop stress to be generated in the former which, when it exceeds the tensile strength of the material, results in radial cracking.

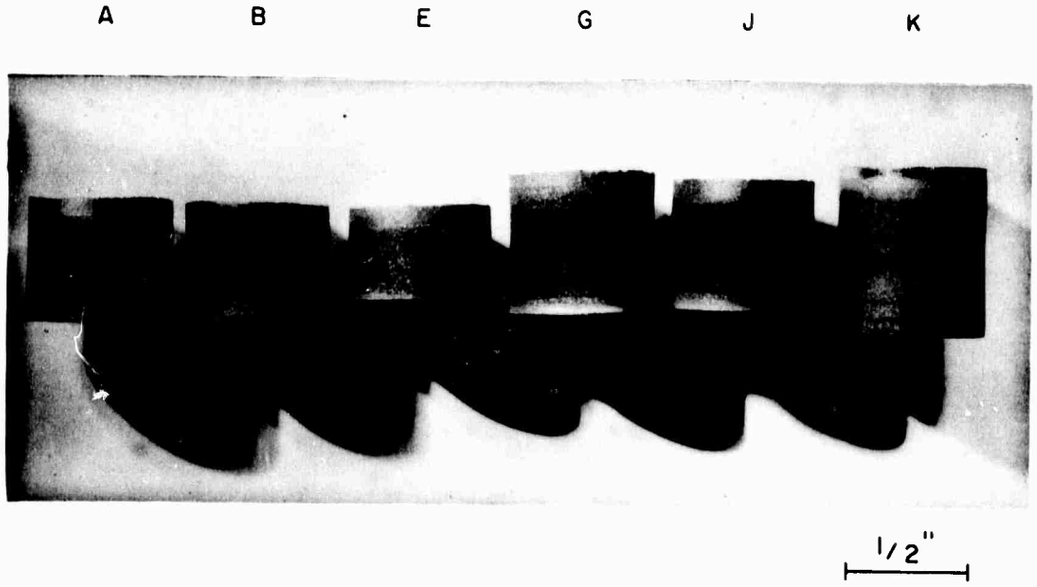

FIGURE 21 Multilayered Insulating Cermet Cylinders

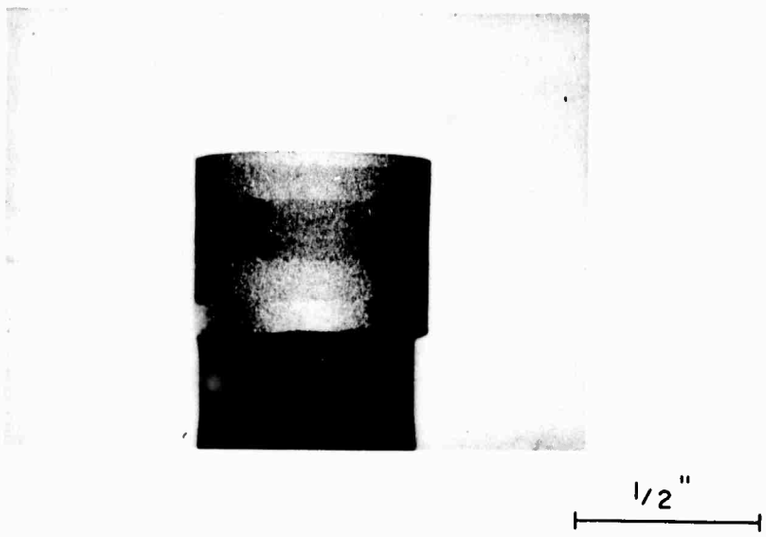

FIGURE 22 Cermet Cylinder Showing Radial Cracks

A typical case of radial cracking is shown in Figure 22 The contrast of the two cracks which are visible in the photograph has been accentuated by a penetrating dye. This cylinder was a seven-layer cermet and the cracks extend across the three central layers; the central 15 v/o molybdenum layer and the adjacent 25 v/o molybdenum layers.

Figure 23 is an attempt to show graphically several examples of composition gradients which develop radial cracks and several which do not. Each figure represents a section through one wall of a hollow, cylindrical, graded cermet structure. The relative proportion of each composition is represented by the thickness of the layer and the identifying numbers represent volume percent molybdenum. The presence of radial or circumferential cracks after several types of testing is shown for each cylinder. Photographs of many of the actual cylinders are shown in Figures 21 and 22.

If one assumes a modulus of elasticity of 40×10^6 pounds per square inch and a tensile strength of 20×10^3 pounds per square inch for an alumina-rich cermet, the strain at failure would be 0.5×10^{-3}. The differential contraction of two adjacent layers in a multilayered cermet causes a strain in each layer upon cooling from the sintering temperature. If it is assumed that strain occurs equally in both layers upon cooling from the 1900°C sintering temperature, the ultimate tensile strength of the higher expansion layer would be reached

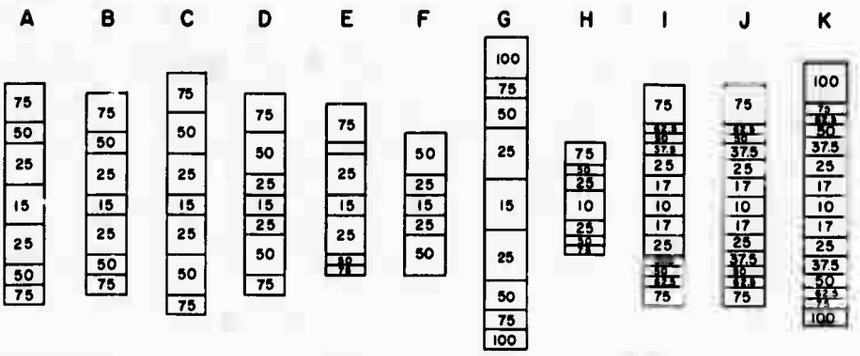

	A	B	C	D	E	F	G	H	I	J	K
AFTER SINTERING	VT	VT	VT	R	VT	R	VT	R	VT	VT	VT
AFTER 9 CYCLES AT 900°C	VT	VT	VT		VT		VT		C	VT	VT
AFTER 327 HOURS AT 1250°C	VT	VT	VT		VT		VT			C	C

NOTES - 1) VT = VACUUM TIGHT, R = RADIAL CRACKS, C = CIRCUMFERENTIAL CRACKS
2) MANY OF THESE STRUCTURES ARE SHOWN IN TWO PRECEEDING FIGURES

FIGURE 23 Graphical Representation of Cermet Composition Gradients Leading to Radial Cracking

at the interface when the differential expansion between the two layers exceeded approximately 0.52×10^{-6} inch per inch per degree centigrade.

Calculated 25°C to 1900°C average expansion coefficients for several compositions are shown in Table 11. The 0.52×10^{-6} differential between layers is met by using compositions which differ in metal content by about 13 v/o.

In compositions which form a continuous metal phase (greater than about 17 v/o metal) or which contain additions of yttrium oxide, the strength is higher and the allowable differential is, therefore, somewhat higher. This, plus the fact that the interface is broad and the stress is not simply as calculated but is affected by the stress at the opposite interface, probably accounts for the excellent high-temperature test results obtained with many cylinders which had as high as 1.0×10^{-6} inch per inch per degree centigrade differential between the 25, 50 and 75 v/o layers.

Cylinders I, J and K of Figure 23 developed circumferential cracks during testing even though they had a favorable grade structure. A polished section of one specimen showed a very desirable, homogeneous structure in each layer and a relatively broad interface zone between layers as a result of the manner in which the granules fell into the die cavity. Failure occurred near, but not directly through, this region between the 17

and 10 v/o molybdenum layer. Although the exact cause of failure was not established, it is possible that a shallow circumferential lamination was present in the sintered piece which did not extend through the wall thickness and, thus, would not have been detected by the helium leak test.

The stress in each layer of a multilayered cermet is, of course, not simply as described previously. In addition to circumferential tension and radial shear at the interface, bending movements cause axial tension. Furthermore, the central insulating layer is sandwiched between layers of lower expansion while all other layers have a higher expansion layer on one side and a lower expansion layer on the other side.

Until practical methods for continuously varying the composition are developed, or until layers of quite uniform thickness can be loaded into a die, it appears necessary to use relatively thick layers in those regions most susceptible to failure -- the central region.

Mechanical Strength of Cermets

The flexural strength of cermet bodies containing from 10 to 100 v/o molybdenum was measured using four point loading. The specimens were rectangular bars approximately 0.200-inch square cross section by 1-1/2 inches long. The sintered bars were diamond ground on opposing sides -- the sides against which the load would be applied.

The data obtained is presented in Table 12 and each value represents the average of a minimum of three (a maximum of six) specimens.

Flexural strength can be seen to increase progressively as the volume fraction of molybdenum in the cermet increases. Strength ranges from 43,000 pounds per square inch for a 10 v/o molybdenum composition to 63,000 pounds per square inch for a 75 v/o composition. Small additions of yttrium oxide significantly increase the mechanical strength of cermet bodies, yielding values ranging from 63,000 pounds per square inch for a 15 v/o molybdenum body to 129,000 pounds per square inch for a 75 v/o molybdenum composition. The strength of a 100 v/o molybdenum specimen was only 96,000 pounds per square inch.

High-Temperature and Thermal-Cycle Testing

Figure 23 contains the results of thermal-cycle and high-temperature (1250°C) testing of hollow, cylindrical, multilayered cermet structures possessing various composition gradients. A photograph of many of these cylinders appears in Figure 21.

The data indicate that structures having a favorable composition gradient are capable of being thermally cycled to temperatures at least as high as 1250°C. Many of the successfully tested cylinders contained adjacent layers whose composition differences were greater than is considered optimum. By reducing the composition gradient a reduction in stress and a consequent increase in "safety factor" should be obtained.

TABLE 3

Sintering Behavior of Cermet Raw Materials

	Density D (g/cc)	Density % Theor.	% Shrinkage	Conductivity[3]
A. Linde A plus MgO as $Mg(OH)_2$				
0.25 w/o	3.969		31.1	
0.60	3.883		31.0	
2.40	3.681		30.3	
5.70	3.364		25.7	
B. A-14, -325 mesh, plus MgO as $Mg(OH)_2$				
0.25 w/o	3.946		22.8	
0.60	3.906		22.7	
2.40	3.737		21.4	
5.70	-		17.7	
C. Cermet, 25 v/o molybdenum; 75 v/o Linde A plus MgO as $Mg(OH)_2$				
0.25 w/o	5.527	99.95	29.1	
0.60	5.489	99.26	28.9	
2.40	5.324	96.27	28.6	
5.70	5.067	91.63	26.6	
D. Cermet, same asIII except MgO as $MgCO_3$				
0.25 w/o	5.537	99.95	29.1	
0.60	5.499	99.45	28.9	
2.40	5.435	98.28	29.1	
5.70	5.240	94.76	28.8	
E. Cermets with varying metal-oxide (A-14 plus 0.25 w/o MgO as $Mg(OH)_2$) ratios				
25 v/o molybdenum	5.465	98.82	24.1	C
20	5.156	98.59	23.5	C
15	4.873	99.25	24.3	N
10	4.576	99.48	23.8	N
5	4.263	99.37	22.8	N

NOTES: (1) All specimens wet mixed in acetone, dried, mixed with binder (isobutyl methacrylate in butyl carbitol acetate), pressed at 10 tons per square inch, sintered at 1900°C for 300 minutes

(2) Molybdenum is M&R, Type P, No. 6856

(3) C = conducting; N = nonconducting

TABLE 4

Effect of Yttria Additions on the Sintering of Cermets

	1716°C for 120 min.		1812°C for 300 min.		1905°C for 300 min.		1930°C for 300 min.	
	D %Theor.	% Shr.	D %Theor.	% Shr.	D %Theor.	% Shr.	D %Theor.	% Shr.
A. A-14 (-325 mesh) plus yttria								
No. 99 - 0.25 w/o yttria	91.0	18.3	92.9	19.1	98.6	-	99.5	22.3
100 - 1.0	92.6	20.1	95.2	20.7	99.0	22.1	99.3	22.3
111 - 2.0	94.1	20.7	97.4	21.7	99.0	22.7	98.4	21.9
112 - 4.0	97.4	21.6	98.3	22.9	96.9	-	96.3	22.5
B. Cermets with varying metal-oxide (A-14 plus 1 w/o yttria) ratios								
No. 107 - 75 v/o molybdenum	94.6	24.1	98.3	27.6	99.3	26.5		
108 - 50	97.6	21.7	98.7	25.4	99.3	25.8		
109 - 25	95.0	20.6	99.4	24.5	99.7	25.0		
110 - 15	94.7	21.9	99.5	23.5	99.3	23.7		

NOTES:

(a) Molybdenum is M&R, Type P, Lot No. 6856

(b) All specimens pressed at 10 tons per square inch and sintered in dry hydrogen

(c) Theoretical densities of compositions 99, 100, 111, and 112 calculated to be 3.98, 3.99, 4.00, and 4.02 grams per cubic centimeter, respectively.

TABLE 5

Shrinkage and Density of Cermets
Containing Yttrium Oxide

Comp. No.	v/o Molybdenum	10 tons/in^2 D % Theor.	10 tons/in^2 Shr. %	20 tons/in^2 D % Theor.	20 tons/in^2 Shr. %
174	100	97.9	25.2	97.3	23.2
170	75	99.1	24.8	99.0	22.1
171	50	99.8	23.9	99.9	21.3
172	25	98.9	23.3	100.1	20.5
173	15	100.2	22.3	100.5	19.9

Notes

All compositions prepared from M & R molybdenum lot No. 7213, Alcoa A-14 (-325 mesh) alumina and Lindsay No. 1115 yttrium oxide.

All compositions contained 1.0 w/o Y_2O_3 based on total oxide content.

All compositions contained 7 w/o paraffin and were milled 1.5 hours in xylene in a pure alumina mill, evaporated to dryness, screened and pressed.

All specimens were sintered 1917°C - 300 min.

Theoretical densities assumed to be 10.220, 8.663, 7.106, 5.548, and 4.925 grams per cubic centimeter, respectively.

TABLE 6

Effect of Organic Binders on Sintering of Powders

	Pressed at 10 tons/in.^{2}		Pressed at 20 tons/in.^{2}	
	D % Theor.	Shr. %	D % Theor.	Shr. %
A. Molybdenum with binder				
No. 121 - No. 6856 with IBM in solvent	98.4	26.9	99.5	20.7
123 - No. 6856 with 2.5% cetyl alcohol	98.6	27.2	99.3	21.1
130 - No. 7234 with 2.5% cetyl alcohol	94.9	25.0	96.3	20.1
136 - No. 7234 with 6.5% cetyl alcohol	93.9	26.2	94.6	22.7
146 - No. 7234 with 3% paraffin	94.0	26.7	96.1	19.3
152 - No. 7234 with 7% paraffin	93.6	26.2	95.1	20.3
B. Alumina with binder, A-14 plus 0.25 w/o MgO				
No. 129 - with 2.5% cetyl alcohol	99.8	23.1	99.6	20.9
135 - with 6.5% cetyl alcohol	99.7	23.1	99.4	21.1
147 - with 3% paraffin	99.8	23.5	-	-
153 - with 7% paraffin	99.5	23.5	99.4	20.7
C. Cermets with binder, molybdenum No. 6856 with A-14 alumina plus 0.25 w/o MgO				
1. - With 2.5% cetyl alcohol				
No. 125 - 75 v/o molybdenum	98.6	27.3	98.7	21.1
126 - 50 v/o molybdenum	99.1	26.9	99.4	22.3
127 - 25 v/o molybdenum	99.1	24.8	99.4	22.3
128 - 10 v/o molybdenum	99.0	23.9	99.3	20.7
2. - With 6.5% cetyl alcohol				
No. 131 - 75 v/o molybdenum	98.4	28.5	98.8	22.5
132 - 50 v/o molybdenum	98.6	27.6	98.4	24.3
133 - 25 v/o molybdenum	98.5	25.2	98.4	24.3
134 - 10 v/o molybdenum	99.2	23.7	99.4	21.7
D. Cermets with binder, molybdenum No. 7234 with A-14 alumina plus 0.25 w/o MgO				
1. - With 3% paraffin				
No. 142 - 75 v/o molybdenum	96.6	25.4	97.1	20.9
143 - 50 v/o molybdenum	97.7	25.4	97.9	20.3
144 - 25 v/o molybdenum	98.6	25.0	99.0	20.5
145 - 10 v/o molybdenum	99.6	24.5	99.6	20.9
2. - With 7% paraffin				
No. 148 - 75 v/o molybdenum	96.1	26.2	96.9	19.5
149 - 50 v/o molybdenum	97.6	25.8	97.8	20.9
150 - 25 v/o molybdenum	99.0	24.3	99.2	20.9
151 - 10 v/o molybdenum	99.6	24.1	99.4	20.7

TABLE 7
Shrinkage and Density of Cermets

Comp. No.	v/o Molybdenum	10 tons/in^2 D % Theor.	10 tons/in^2 Shr. %	20 tons/in^2 D % Theor.	20 tons/in^2 Shr. %	Conducting (C) or Nonconducting (N)
156	75.0	95.8	25.8	97.0	22.9	C
157	62.5	97.3	23.7	98.0	21.7	C
158	50.0	99.5	24.5	99.8	21.8	C
159	37.5	98.7	23.5	100.0	20.9	C
160	25.0	100.0	22.9	100.2	20.3	C
161	17.0	100.8	22.5	100.7	20.5	N
162	10.0	100.6	22.3	100.8	20.3	N

Notes

All compositions prepared from M & R molybdenum lot No. 7213 and Alcoa A-14 alumina (-325 mesh). All contained 0.12 w/o MgO added as magnesium carbonate, and 7 w/o paraffin.

All compositions milled 3 hours in xylene in a pure alumina mill, evaporated to dryness, screened and pressed.

All specimens sintered 1909°C - 300 min in dry hydrogen.

Theoretical densities calculated to be 8.660, 7.880, 7.100, 6.320, 5.540, 5.041, and 4.595 grams per cubic centimeter, respectively (156 through 162).

TABLE 8

Shrinkage and Density of Cermets
Containing Linde A Alumina

Comp. No.	v/o Molybdenum	10 tons/in^2 D % Theor.	Shr. %
182	75	99.5	28.4
183	50	98.5	27.7
184	25	100.6	27.8
185	10	101.3	27.6

Notes

All compositions prepared from M & R molybdenum lot No. 7213 and Linde A alumina. All contained 0.12 w/o MgO added as magnesium carbonate, and 7 w/o paraffin.

All compositions milled one hour in xylene in a pure alumina mill, evaporated to dryness, screened and pressed.

All specimens sintered 1906°C - 300 min.

TABLE 9
Shrinkage and Density of Cermets
Containing a Blend of Aluminas

Comp. No.	v/o Molybdenum	10 tons/in^2 D % Theor.	10 tons/in^2 Shr. %	20 tons/in^2 D % Theor.	20 tons/in^2 Shr. %
165	75	98.1	24.5	97.7	23.1
166	50	97.2	23.7	97.2	21.1
167	25	99.6	21.9	99.4	19.1
168	10	100.1	22.5	100.1	21.7

Notes

All compositions prepared from M & R molybdenum lot No. 7213, Alcoa A-14 (-325 mesh) alumina, and Linde A alumina.

All compositions contained 80 w/o A-14 and 20 w/o Linde A alumina.

All compositions contained 0.12 w/o MgO added as magnesium carbonate, and 7 w/o paraffin.

All compositions milled 3 hours in xylene in a pure alumina mill, evaporated to dryness, screened and pressed.

All specimens sintered 1909°C - 300 min.

Theoretical density calculated to be 8.660, 7.100, 5.540, and 4.595, respectively.

TABLE 10
Shrinkage and Density of Cermets

Comp. No.	v/o Molybdenum	10 tons/in^2 D % Theor.	10 tons/in^2 Shr. %
177	100	97.4	25.1
178	75	99.6	26.1
179	50	100.3	25.6
180	25	100.5	25.0
181	10	100.8	23.8

Notes

All compositions prepared from M & R molybdenum lot No. 7213, and Alcoa A-14 (-325 mesh). All contained 0.12 w/o MgO added as magnesium carbonate, and 3.5 w/o paraffin.

All compositions milled 1 hour in xylene in a pure alumina mill, evaporated to dryness, screened and pressed.

All specimens sintered 1906°C - 300 min.

TABLE 11
Calculated Expansion Coefficients

Molybdenum-Alumina Cermet Composition v/o Molybdenum	Calculated Thermal Expansion Coefficient in./in./^{o}C, RT to 1900^{o}C
100	6.68
75	7.71
62.5	8.23
50.0	8.74
37.5	9.26
25	9.77
15	10.18

TABLE 12
Flexural Strength of Cermets

Comp. No.	v/o Molybdenum	Flexural Strength psi	Percent Shrinkage	Conducting (C) or Nonconducting (N)
156	75.0	72,600	24.1	C
157	62.5	71,900	22.8	C
158	50.0	61,000	23.5	C
159	37.5	62,200	22.1	C
160	25.0	59,800	21.7	C
161	17.0	54,500	21.8	N
162	10.0	42,600	21.5	N
165	75.0	110,600	23.7	C
166	50.0	69,600	23.2	C
167	25.0	60,400	22.0	C
168	10.0	47,400	22.4	N
174	100	96,100	24.3	C
170	75	129,300	23.6	C
171	50	67,600	23.6	C
172	25	58,600	22.9	C
173	15	63,100	22.2	N

Note

All specimens pressed at 15 tons per square inch and sintered 1917°C - 300 minutes

Conclusions

1. Molybdenum-alumina cermets containing from 10 to 100 v/o molybdenum can be sintered to densities in excess of 98 percent of theoretical to achieve strong, vacuum-tight bodies.

2. Small additions of yttrium oxide aid densification and mechanical strength.

3. Techniques for the fabrication of multilayered, hollow cermet cylinders have been developed and critical parameters have been identified. Homogeneity of composition, the use of an effective organic binder and lubricant, and the attainment of uniform axial pressure during double-action pressing are necessary to prevent lamination before or during sintering. A carefully designed composition gradient is necessary to prevent radial cracking through the central layers during thermal cycling.

4. Multilayered cermet cylinders possessing various composition gradients remained vacuum tight after nine thermal cycles to 900°C followed by 327 hours at 1250°C.

5. The flexural strength of the cermet compositions which comprise a typical multilayered cermet structure range from 43,000 pounds per square inch for a 10 v/o molybdenum - 85 v/o alumina composition to 63,000 pounds per square inch for a 75 v/o molybdenum - 25 v/o alumina body.

6. Small additions of yttrium oxide to molybdenum-alumina cermet compositions significantly increase the mechanical strength of sintered bodies. Flexural strength ranges from

63,000 pounds per square inch for a 15-v/o molybdenum body to 129,000 pounds per square inch for a 75 v/o molybdenum composition.

Sub-task C-3 - Metal-to-Metal Joining

Introduction

The objective of this sub-task was the development of processes for joining metallized ceramics or cermets to the structural metal members of thermionic converters.

It was initially anticipated that molybdenum would be the metallic constituent of the surface layer of a multilayered cermet or metallized ceramic. However, when tungsten metallizing exhibited superior strength, almost all subsequent development was with tungsten-metallized ceramics.

The structural metal members or conductor portions of the metal-to-ceramic seal require, by present and anticipated service temperatures, fabrication from molybdenum, niobium, tantalum, tungsten, or their alloys. Therefore, effort was limited to the problem of joining unalloyed molybdenum and tungsten to themselves, in combination, and to unalloyed niobium or tantalum.

As previously discussed,[1] the mechanical strength of the metal-to-metal joint was not the primary concern; rather the following properties were considered of prime importance:

a. Stability (leak tight) at the desired operating temperatures
b. Resistance to cesium corrosion
c. Freedom from brittle phases.

The thinness of the metallic layer on the surface of the ceramic insulators makes the use of inert arc or electron beam welding unattractive as a joining method. Thus, this study was limited almost completely to brazing and modified brazing techniques.

One technique that received attention was reactive (alloying) brazing. Here, a metal added to the joint reacts with the structural members, forming a composition that melts at a temperature below the melting point of the added metal. Subsequent holding at this temperature or at a higher temperature, may then be used to further change the composition of the material in the joint (by diffusion) and cause the melting point to increase to a value above the operating temperature. This complete technique, termed "braze-diffusion-bonding", offered considerable promise at a test temperature of 1000°C when using nickel as the braze-diffusion-bonding material. In fact, it was previously shown[1] that it is feasible to bond molybdenum to molybdenum-metallized alumina ceramics without destroying the metallizing, and that the bond so formed is almost completely free of an interface layer when using very thin nickel (0.0001 inch).

Brazing by means of the braze-diffusion-bonding technique, however, appears to be limited to butt joints where a very thin shim of the braze material can be preplaced. For concentric type joints, preplacement of the braze material in the joint is not normally feasible, nor is the application of uniform pressure to limit joint clearance. Therefore, a flow-type braze is needed. Although the braze-diffusion-bonding principle can be used to develop a sound bond, flow-type brazing places an additional

requirement on the braze material, since there must be good flow into the joint. Also, the flow temperature must be established by the braze itself, because relying on reaction with the structural members to develop a low melting point may consume too much of the structural members at the point where the braze material is applied.

The considerations used in the selection of materials for flow-type brazing were previously discussed.[2] The metals selected were chromium, iron, nickel, niobium and palladium. No attempt was made to optimize the composition of those metal combinations found potentially useful.

Since a graded cermet can be graded all of the way to 100 percent metal, electron beam welding may offer a technique for joining this type of structure to a metal member. Consideration was, therefore, given to this technique but a complete investigation was not attempted.

Experimental Procedure

The procedures used for braze-diffusion-bonding and flow brazing have been previously discussed.[2] All electron beam welding was done between 1/2-inch diameter by 1/16-inch thick cermet discs, containing 25 v/o ceramic, and molybdenum sleeves of the same diameter having a wall thickness of about 0.040 inch. Only the beam position and the amount of preheat and precool were varied.

Results and Discussion

a. Nickel braze-diffusion-bonding

Unfortunately, the parameters[2] suitable for nickel braze-diffusion-bonding niobium to molybdenum did not produce desirable results when attempting a bond to tungsten-metallized alumina ceramics. As shown in Figure 24, not only has the tungsten in the metallizing been highly densified, but the interface appears to have moved into the niobium and become completely saturated with pores. Figure 24 also shows the bonds obtained with molybdenum to niobium (rather than tungsten-metallized alumina to niobium) using a similar nickel braze-diffusion-bonding cycle. Note the complete absence of porosity and very limited reaction with molybdenum.

It was subsequently determined that the tungsten and not the metallizing, as such, caused the pores. A possible explanation for this effect is the lower solubility of nickel in tungsten. During bonding, the nickel is not absorbed into the tungsten, whereas the niobium, which is completely soluble, is absorbed, thus continually exposing the high nickel liquid to fresh (relatively pure) niobium. Since considerable liquid (but not as a uniform layer) is present when cooling begins, the shrinkage that occurs when going from liquid to solid causes pores at the joint. Attempts to prevent this effect by using very thin (<0.00005 inch) nickel plating were unsuccessful. Incomplete bonding occurred because of insufficient liquid to nullify surface irregularities, and in those areas where contact was made, pores still formed.

NIOBIUM WASHER

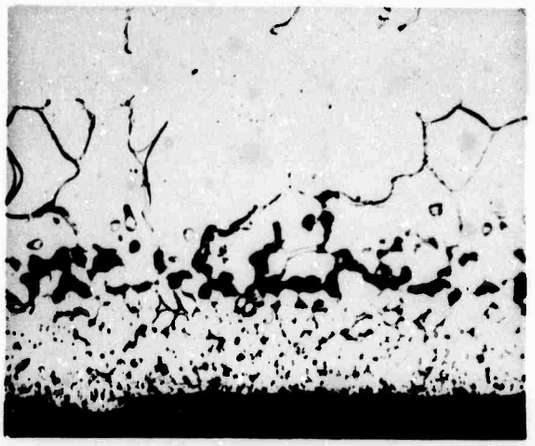

45 ANCNA
1500°C, 2 MIN.
NO. 60 METALLIZING

CERAMIC

NIOBIUM WASHER

2 MNCNM
1610°C, 2 MIN.

MOLYBDENUM RING

FIGURE 24 Nickel Braze-Diffusion-Bonded to Tungsten Metallizing and Molybdenum (250X)

As shown in Figure 25, the parameters found suitable for nickel braze-diffusion-bonding tantalum to molybdenum[2] were not completely effective in producing sound leak-tight bonds when bonding tantalum to tungsten-based metallizing. Going to still higher temperatures resulted in almost a complete interface of pores. For comparison, photomicrographs of nickel braze-diffusion-bonded tantalum to molybdenum containing metallizing and to solid molybdenum are also shown in Figure 25. Note the complete absence of porosity.

As with niobium and tantalum, the parameters found suitable for nickel braze-diffusion-bonding molybdenum to molybdenum have been previously discussed.[2] Although pores do not appear to develop when nickel braze-diffusion-bonding molybdenum to tungsten-based metallizing, more nickel intermetallic appears to form and seems to penetrate the molybdenum-grain boundaries more than when bonding molybdenum to molybdenum. This effect is shown in Figure 26 where the 0.005-inch thick molybdenum washer was completely penetrated by the intermetallic. Also shown in Figure 26 is a photomicrograph of a similar bond which was made by applying the nickel as a plating on the molybdenum washer rather than as a shim. The fractures in the ceramics illustrates the high residual stresses caused by the large thermal expansion mismatch between molybdenum and alumina ceramic.

Some very excellent appearing bonds were obtained when nickel braze-diffusion-bonding tungsten to tungsten metallizing. As shown in Figure 27, a temperature of about 1600°C and holding period of about 2 minutes produced bonds that

TANTALUM WASHER

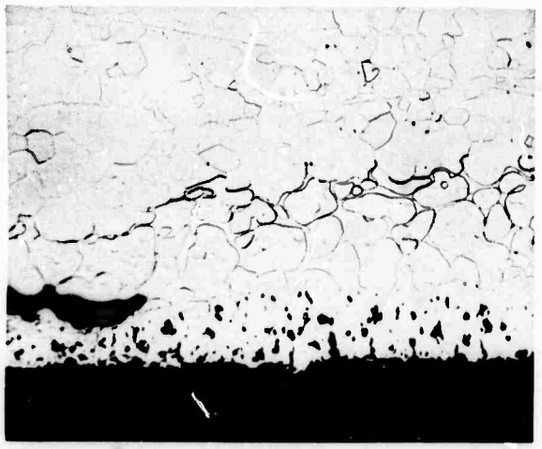

27 ANTNA
1620°C, 2 MIN
NO. 155 METALLIZING

CERAMIC

TANTALUM DISC

21 TNA
1610°C, 1 MIN
NO. 36 METALLIZING

CERAMIC

TANTALUM DISC

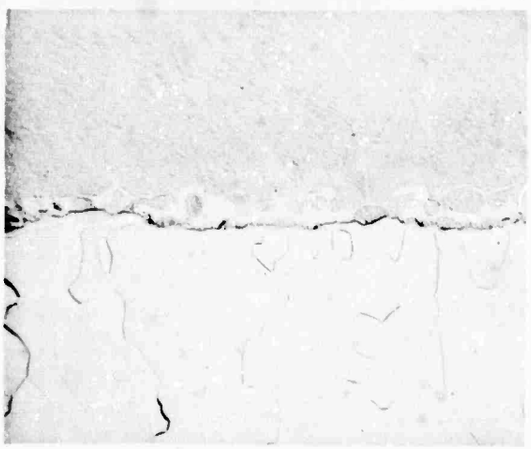

19 TNM
1610°C, 1/2 MIN

MOLYBDENUM RING

FIGURE 25 Tantalum Nickel Braze-Diffusion-Bonded to Tungsten and Molybdenum Metallizing and to Molybdenum (250X)

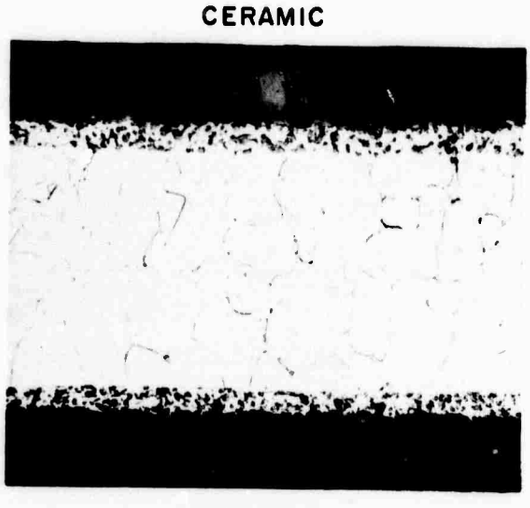

MOLYBDENUM WASHER
69 ANMNA
1510°C, 2 MIN.
NO. 155 METALLIZING

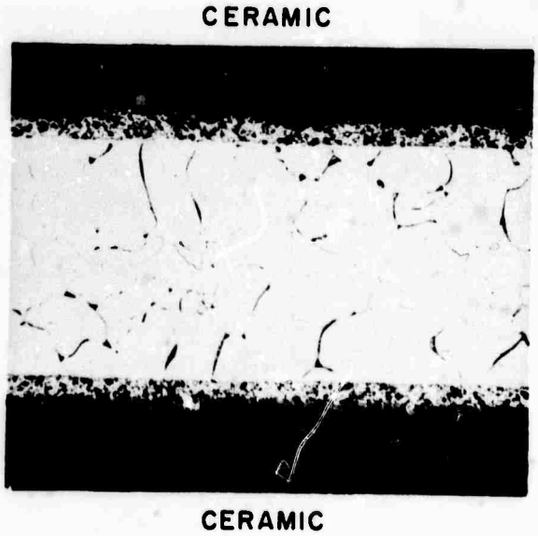

76 ANMNA
1510°C, 2 MIN.
NO. 155 METALLIZING
NICKEL PLATING

FIGURE 26 Molybdenum Nickel-Braze-Diffusion Bonded to Tungsten Metallizing (250X)

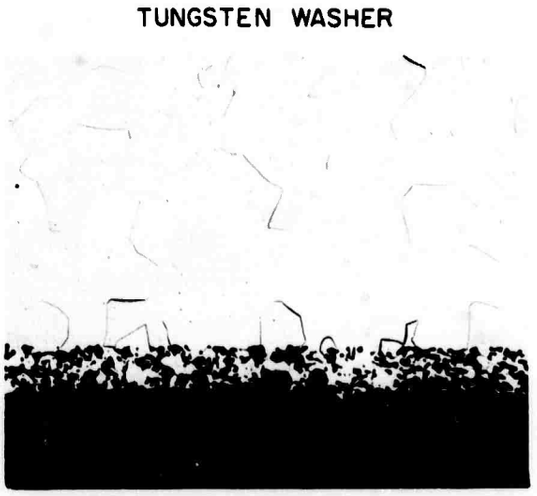

FIGURE 27 Tungsten Nickel Braze-Diffusion-Bonded to Tungsten Metallizing (250X)

were almost completely free of pores and intermetallics. Because of the poor thermal expansion match between tungsten and alumina ceramic, however, almost all seals leaked "as brazed" due to cracking of the ceramics. No attempt was made to minimize thermal stresses by use of thinner tungsten (less than 0.010 inch) or by cooling very slowly.

b. Flow brazing

The flow braze compositions selected for study, along with their estimated flow temperatures, are listed in Table 13*. The initial evaluation of these compositions has been previously discussed.[2] There was little additional study given to flow braze alloys I, II, IV, VI and VIII for the following reasons:

Braze I (50 w/o Cr - 50 w/o Ni) exhibited a tendency to form brittle phases. While these brittle phases could be inhibited by holding at higher temperatures (about 1600°C), considerable reaction by the braze occurred with niobium and tantalum at these higher temperatures and there was a tendency toward pore formation with molybdenum. Also the level of reaction that occurs with molybdenum was believed too extensive for successful sealing to molybdenum-based metallizing.

Braze II (22 w/o Cr - 78 w/o Fe), like braze I, exhibited a tendency towards brittle phase formation with molybdenum and tantalum, and there was considerable penetration into niobium. Brazing at a higher temperature (1650°C or higher) might possibly have minimized the brittle phase formation with molybdenum and tantalum, but effort was transferred to other more promising compositions.

*Table 13 appears on page 81

Braze IV (59.4 w/o Cr - 40.6 w/o Pd) in some respects is quite similar to braze III (to be discussed under promising compositions), but did not appear to flow into the joint as well and appeared to have more of a reaction with molybdenum. The complete solid solubility of chromium in molybdenum and the higher chromium content in braze III may account for the greater reaction with molybdenum.

Braze VI (20 w/o Cr - 48 w/o Pd - 32 w/o Ni) is similar to brazes I and II since there is a tendency towards brittle phase formation and, at higher temperatures the penetration into niobium becomes excessive. At about 1500°C, the bond obtained between molybdenum and molybdenum does, however, approach that obtained with nickel braze-diffusion-bonding.

Braze VIII (34 w/o Nb - 33 w/o Cr - 33 w/o Ni) did not consistently exhibit good flow and showed a tendency towards brittle phase formation with tantalum and molybdenum. However, with niobium, when complete flow was realized, bonds similar to those obtained by proper nickel braze-diffusion-bonding were obtainable. Brazing at higher temperatures (above 1500°C) could possibly be effective in eliminating brittle phases in the tantalum to molybdenum and molybdenum to molybdenum bonds, and might possibly improve the flow.

The other three braze compositions, III, V and VII, exhibited quite promising results and, therefore, received considerable study. The attributes and limitations of these brazes are discussed in the following paragraphs.

Braze III (38 w/o Cr - 62 w/o Pd) produced its best appearing bonds when bonding molybdenum to molybdenum and to tungsten. Although these bonds were obtainable at 1500°C, holding for 2 minutes at 1600°C caused no appreciable change (Figure 28). Increasing the brazing temperature from 1500 to 1600°C for niobium to molybdenum, however, caused the good appearing bond to change to a porous structure. Similar results were obtained with tantalum to molybdenum, but the brittle layers, developed on the tantalum at 1500°C, were transformed into a dispersed brittle phase at the higher temperature. Also shown in Figure 28 is a bond formed between tungsten and tungsten-based metallizing by brazing at 1500°C. Although the bond is completely intact and pore free, the ceramic is severely cracked from stresses caused by the poor thermal-expansion match between tungsten and the alumina ceramic. No attempt was made to minimize these stresses.

Braze V (50 w/o Nb - 30 w/o Pd - 20 w/o Ni) also formed good appearing bonds when brazing molybdenum to molybdenum, molybdenum to tungsten, and tungsten to tungsten (Figure 29). Good bonds were also obtained when brazing tantalum and niobium to molybdenum. However, at a 1500°C braze temperature, considerable reaction can occur between the braze and the niobium or tantalum if an excess amount of braze is present. When brazing niobium or tantalum to tungsten-based metallizing, pores form at the interface in a manner similar to nickel braze-diffusion-bonding.

MOLYBDENUM DISC

4 M III M
1605°C, 2 MIN.

MOLYBDENUM RING

TUNGSTEN WASHER

1 W III M
1605°C, 2 MIN

MOLYBDENUM RING

TUNGSTEN WASHER

3 A III W III A
1500°C, 2 MIN.
NO. 73 METALLIZING

CERAMIC

FIGURE 28 Bond Structures Formed with Braze III (250X)

MOLYBDENUM DISC

3 M V A
1490°C, 1.5 MIN
NO. 36 METALLIZING

CERAMIC

MOLYBDENUM WASHER

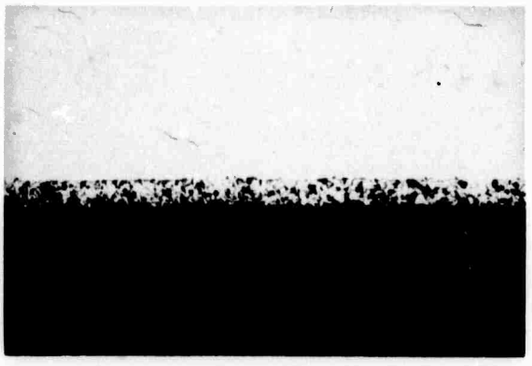

21 A V M V A
1500°C, 2 MIN
NO. 155 METALLIZING

CERAMIC

TUNGSTEN WASHER

6 A V W V A
1505°C, 1 MIN
NO. 73 METALLIZING

CERAMIC

FIGURE 29 Bond Structures Formed with Braze V (250X)

Braze VII (67 w/o Nb - 33 w/o Fe) was almost discarded because of the brittle phase cracking problem when brazing molybdenum to molybdenum. However, this problem was eliminated without significant increase in reaction with niobium, tantalum or molybdenum by increasing the brazing temperature to 1670°C and higher. This is illustrated in Figure 30 which also shows a braze made between tungsten and molybdenum that is crack free but in which some pores did develop. As shown in Figure 31, such pores did not form when brazing molybdenum to tungsten-based metallizing. Also note in Figure 31 the limited densification of the tungsten in the metallizing compared to that which occurs when brazing to niobium (Figure 31). Densification is probably undesirable because of the loss of interlocking or mechanical bonding between the metal coating and the ceramic. Pore formation, similar to that which occurs with nickel braze-diffusion-bonding, occurred with niobium (and to a lesser extent with tantalum) when brazing to tungsten metallizing, but to a much lesser degree than when nickel braze-diffusion-bonding niobium to tungsten. Braze VII was also found to be capable of forming leak-tight seals to bare ceramic as an active alloy type braze. However, these bonds were quite weak -- apparently from the lack of mechanical interlocking that is obtained from a preplaced metallizing.

c. Ultra-high-temperature brazing

The use of ultra-high-temperature braze materials specifically designed for use with refractory metal and alloys has been previously discussed.[1, 2, 3] Under Contract NObs-88578

TABLE 13

Flow-Braze Compositions

Braze No.	Composition (weight percent)	Estimated Flow Temperature (°C)
I	50 Cr - 50 Ni	1345
II	22 Cr - 78 Fe	1507
III	38 Cr - 62 Pd	1300
IV	59.4 Cr - 40.6 Pd	1320
V	50 Nb - 30 Pd - 20 Ni	1230
VI	20 Cr - 48 Pd - 32 Ni	1130
VII	67 Nb - 33 Fe	1560
VIII	34 Nb - 33 Cr - 33 Ni	1400

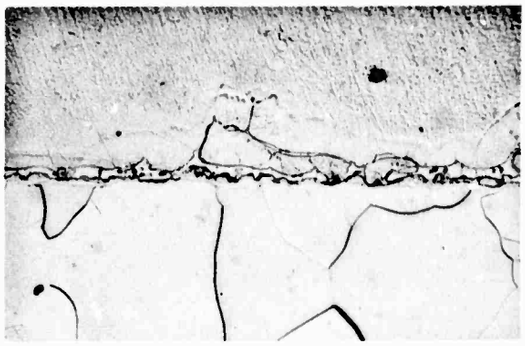

4C VII M
1670°C, 1/2 MIN.

MOLYBDENUM RING

TANTALUM DISC

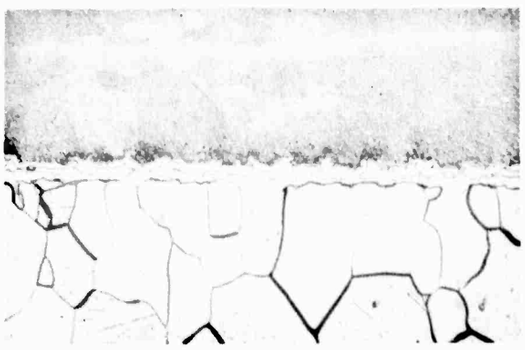

4T VII M
1670°C, 1/2 MIN.

MOLYBDENUM RING

MOLYBDENUM DISC

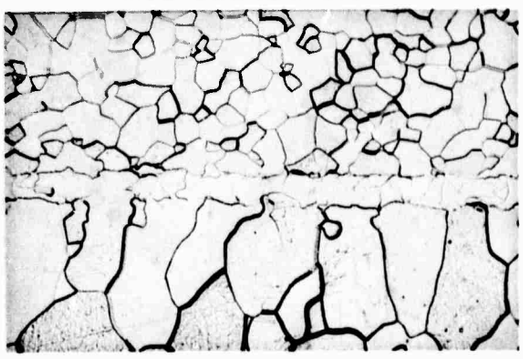

4M VII M
1670°C, 1/2 MIN.

MOLYBDENUM RING

TUNGSTEN WASHER

1W VII M
1670°C, 1/2 MIN

MOLYBDENUM RING

FIGURE 30 Bond Structures Formed with Braze VII (250X)

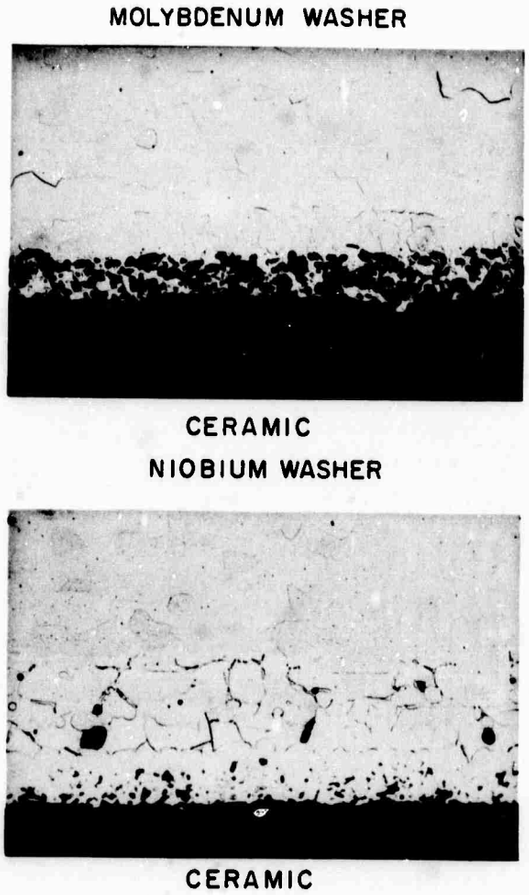

1 A VII M VII A
1670°C, 1 MIN.
NO. 115 METALLIZING

13 A VII C VII A
1680°C, 2 MIN.
NO. 60 METALLIZING

FIGURE 31 Bond Structures Formed with Braze VII (250X)

some of the alloys having a high content of vanadium, titanium and zirconium were shown to be resistant to cesium at 1000°C. Therefore, attempts were made to braze niobium, tantalum, and molybdenum to molybdenum using these materials, which have melting points ranging from about 1700°C to 1870°C. In general, poor flows were obtained and sections taken after test indicated oxidation of the braze layer, from apparent gettering by V, Ti and Zr of the oxygen liberated from the dissociating alumina vessel and baffles. No further attempts were made to isolate the seals from the vessel and baffles and no attempts were made in applying these braze materials to bare or metallized alumina ceramics.

d. Electron beam welding

Three attempts were made to electron beam weld 25 v/o alumina-molybdenum cermet discs to pure molybdenum sleeves by aiming the beam parallel to the butt joint. The excellent bonding that was obtained between the cermet and the molybdenum is illustrated in Figure 32. Globs of alumina, which melts at a lower temperature than molybdenum, formed in the weld and on the weld surface. Keeping the beam on the molybdenum side of the joint did not completely eliminate this effect. Although all of the specimens leaked, they did not do so from pores in the joint or from cracking of the cermet, but rather from cracking of the recrystallized molybdenum near the weld. This cracking was undoubtedly caused by thermal stresses which could possibly be eliminated by proper preheating and cooling after welding.

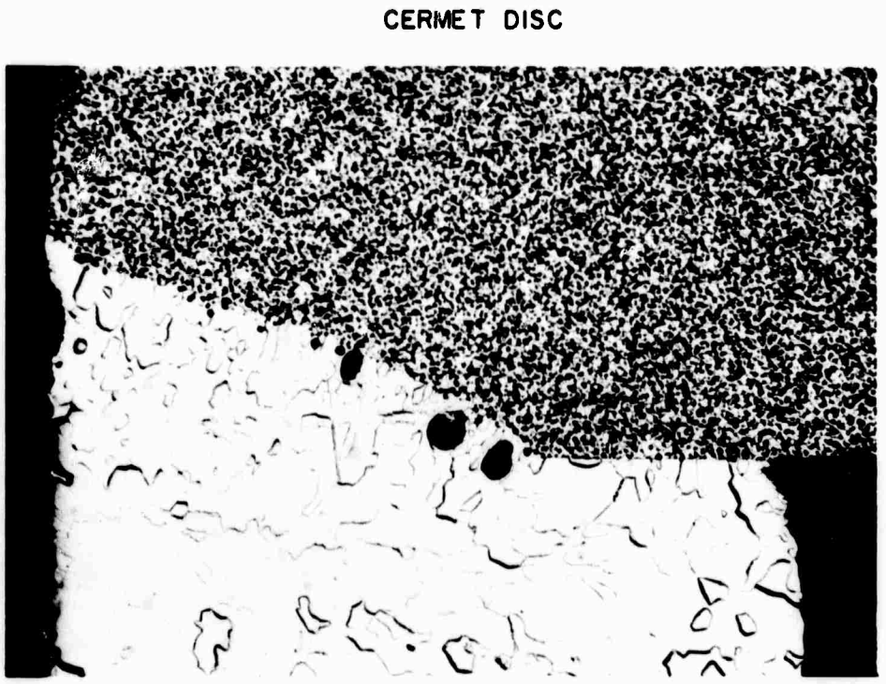

FIGURE 32 Electron Beam Weld Between Cermet Disc and Molybdenum Sleeve (100X)

Conclusions

1. Nickel braze-diffusion-bonding can provide excellent bonding between niobium and molybdenum (as a solid part or as in a metallized surface), between tantalum and molybdenum, molybdenum and molybdenum, molybdenum and tungsten, and tungsten and tungsten. Varying degrees of porosity occur at the interface when attempting to use this technique for bonding niobium or tantalum to tungsten.

2. Braze III can form excellent bonds between molybdenum and molybdenum or tungsten, and between tungsten and tungsten. Good bonds can also be formed between niobium and molybdenum, providing the brazing temperature does not greatly exceed 1500°C.

3. Braze V can provide excellent bonding between molybdenum and molybdenum, molybdenum and tungsten, and tungsten and tungsten. Good bonds are also possible between niobium or tantalum and molybdenum, providing excess braze is not used.

4. Braze VII can also provide excellent bonding between molybdenum and molybdenum, molybdenum and tungsten, niobium and molybdenum and tantalum and molybdenum. There is some tendency towards pore formation when bonding niobium to tungsten.

5. Bonding of niobium or tantalum structural members to molybdenum or tungsten-based metallized alumina ceramics results in considerable densification of the metal in the metallizing.

6. Electron beam welding appears to be a useful technique for bonding graded insulating cermets to the conducting structural members.

Sub-task C-4 - Cesium and Vacuum Life Testing

Introduction

The purpose of this sub-task was: (1) to obtain design data on the resistance of various materials (both insulators and conductors) to attack by cesium vapor; (2) to study the attack on metal-to-metal and metal-to-ceramic seals that are designed for exposure to elevated temperatures (up to 1500°C), and (3) to determine, by testing in vacuum, whether changes that occur in cesium are a function of the cesium or the temperature.

Testing at temperatures as high as 1500°C is desirable for determining the temperature limitations of promising sealing techniques. Also, because of the rapid increase in reaction rates with temperature, testing at 1500°C permits detection in a relatively few hours of undesirable phenomena that might take many thousands of hours to detect at lower temperatures.

Experimental Procedures and Equipment

The test equipment and procedures have been previously discussed.[2] When testing at 1500°C, various techniques were tried in an attempt to minimize oxygen pickup by the specimens (especially niobium and tantalum). The oxygen, which probably originates from the dissociation of the alumina vessel and baffles at the 1500°C temperature, could not be removed fast enough to prevent reaction with the specimens even with continuous pumping.

Some improvement was obtained by wrapping the stem of the hottest baffle with molybdenum and then titanium which acted as a getter. The molybdenum was used to prevent titanium from coming into direct contact with the alumina baffle. A closed-end molybdenum

tube, made from molybdenum sheet, was then used inside of the alumina vessel and molybdenum baffles were substituted for the alumina baffles. This procedure, which was done in an attempt to prevent the oxygen from having direct access to the specimens, did appear to provide some protection. In an attempt to provide still greater protection, the molybdenum cylinder was lined with zirconium. However, the eutectic temperature for molybdenum-zirconium is very near the test temperature, and, as a result, considerable fusion occurred between the two metals. This reaction also caused considerable etching of the ceramics on the seal specimens, but did not appear to effect the seal bonds. In addition, large deposits of aluminum metal were found in the cooler end of the vessel. Finally, the specimens were wrapped in molybdenum foil, then tantalum foil, and then again with molybdenum foil. This scheme gave excellent protection with only minor deposits of aluminum being produced at the cooler end of the vessel.

Because of the difficulties in finding adequate specimen protection, and because of the apparent continuation of braze-base metal reactions at 1500°C, some testing was carried out as low as 1200°C. Although 1200°C is rather low, it was the highest that could be readily obtained from wound, air operating, resistance elements.

Results and Discussion

a. General

As discussed in the semi-annual report, several types of failures, resulting in loss of a pure cesium vapor atmosphere,

were encountered in testing at 1500°C. This included leaks which developed in the tubulation pinch-off and in the alumina vessels after many hours of testing, apparently due to corrosion.

Vessels made from body A-976, an essentially pure polycrystalline alumina containing a small amount of MgO as a grain growth inhibitor, were found to develop porosity in the hot end after several hundred hours of testing with an internal cesium partial pressure of 20 Torr. Microscopic examination of polished sections, as well as x-ray microprobe and silica analyses were performed in an attempt to identify the cause of failure. Examination of polished sections revealed small patches of a grain boundary phase which, by x-ray microprobe analysis, were found to contain silicon.

The quantitative silica analyses which were performed are, however, believed to be unreliable. Analyses of several specimens of A-976 showed silica contents of 0.05 to 0.11 w/o. Analysis of a piece of Lucalox yielded the figure of 0.08 w/o SiO_2. Lucalox is prepared from an ultra-pure alpha alumina, and it seems unlikely that this amount of contamination would have been introduced during processing. Furthermore, no second phase particles have been seen in Lucalox specimens and Lucalox test vessels did not develop porosity on 1500°C cesium testing.

It is believed that failure of A-976 vessels at 1500°C is the result of corrosion of a grain boundary phase (possibly a thin "film") resulting in the development of porosity through the

wall. None of the A-976 vacuum test vessels failed during 1500°C testing even after 1300 hours exposure.

It appears that the purity of alumina ceramics intended for use in 1500°C cesium vapor must be much better than previously believed. Various workers in the field have reported tolerable silica levels ranging from 0.1 to 1.0 w/o. It now appears that silica in excess of about 50 ppm (0.005 w/o) would be undesirable.

b. Nickel braze-diffusion-bonding

Some of the tests that gave the most significant results, along with a tabulation of those results are given in Table 14*. All of those seals with one or two N's in their designation were bonded by nickel braze-diffusion-bonding. The letter "C" in the designation represents niobium (columbium); T, tantalum; M, molybdenum, and W, tungsten with A representing alumina ceramic.

As illustrated in Figure 33, the bonds obtained with niobium nickel braze-diffusion-bonded to molybdenum or molybdenum-based metallizing are essentially unaffected when testing at 1200°C. The difference in the appearance of this bond and the "as brazed" condition shown in Figure 24 is only due to different etching techniques. At 1500°C, and irrespective of whether in a vacuum or cesium vapor, bonds to molybdenum and molybdenum containing metallizing do remain well intact, but some pores do form and there is complete solutioning (dissolving) of the intermetallic second phase. With tungsten

*Table 14 appears on page 95

NIOBIUM DISC

CERAMIC

30 CNA
NO. 36 METALLIZING
TESTED: 1200°C
686 HRS., VAC

TANTALUM WASHER

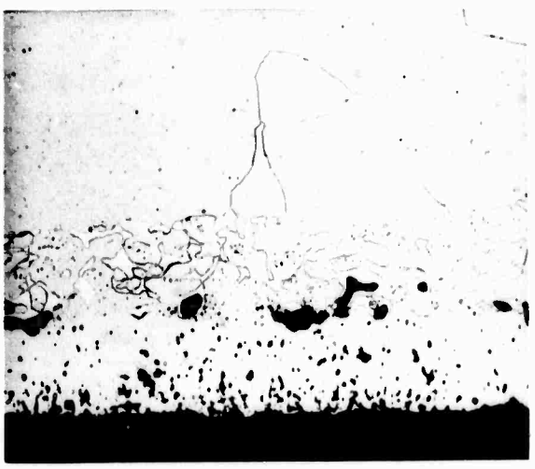

CERAMIC

31 ANTNA
NO. 154 METALLIZING
TESTED: 1500°C
400 HRS., VAC

FIGURE 33 Niobium and Tantalum Nickel Braze-Diffusion-Bonded to Metallized Alumina Ceramic, After Test (250X)

metallizing successful bonding was not realized, as previously discussed and, therefore, no test results were obtained.

Tantalum to molybdenum or molybdenum-based metallizing bonds, formed by nickel braze-diffusion-bonding, were also essentially unaffected after testing at 1200°C. Figure 33 also shows that very little change occurs at 1500°C, from the "as bonded" condition (Figure 25) when bonding to tungsten-based metallizing. The pores are believed to have originated from the bonding operation and not from testing. With molybdenum metallizing, the intermetallic in the joint is almost completely solutioned and the interface boundary between the tantalum and molybdenum disappears during testing at 1500°C.

With molybdenum nickel braze-diffusion-bonded to molybdenum-based metallizing, a very small amount of porosity developed when testing at 1500°C in cesium vapor or vacuum. This limited porosity is believed a result of the very small amount of remaining nickel intermetallic being molten at the testing temperature. With tungsten metallizing, a considerable amount of porosity is formed as illustrated in Figure 34. These much larger pores are believed due to the much larger amount of intermetallic formed during bonding. Although the pores shown in Figure 34 do not appear detrimental to the bond, they have on occasion been found segregated to the metal-metallizing interface with almost complete loss of bonding. At 1200°C essentially no changes occurred in the bond microstructures.

MOLYBDENUM WASHER

CERAMIC

61 ANMNA
NO. 155 METALLIZING
TESTED: 1500°C
230 HRS., Cs

TUNGSTEN WASHER

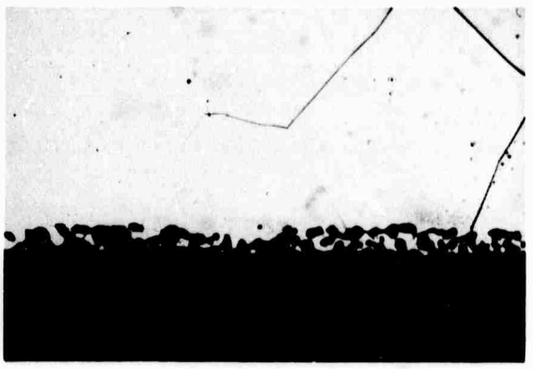

CERAMIC

9 ANWNA
NO. 73 METALLIZING
TESTED: 1500°C
230 HRS., Cs

FIGURE 34 Molybdenum and Tungsten Nickel Braze-Diffusion-Bonded to Metallized Alumina Ceramic, After Test (250X)

With tungsten nickel braze-diffusion-bonded to tungsten metallizing no intermetallic phase was detected (Figure 27) and, therefore, no pore formation would be expected. This was almost true as illustrated in Figure 34. Only a small number of pores appear to have formed at the metal-metallizing interface. Unfortunately, cracking of the ceramics from the poor thermal expansion match ruled out leak checking the integrity of the bonds. As with a molybdenum metal member, considerable densification of the metallizing does occur at 1500°C, whereas no noticeable change occurs at 1200°C. This densification (or continued sintering of the metallizing) is undoubtedly activated by the small amount of nickel present, since negligible sintering occurs when the metallizing is tested by itself as is illustrated in "Sub-task C-1 - Cesium-Resistant Metallizing".

Figure 35 shows the nickel braze-diffusion-bonds between an alumina-molybdenum cermet and a molybdenum washer, and between the washer and a molybdenum ring after testing at 1500°C. Just a few small pores remain at either interface with grain growth across the interface. The lesser volume of pores here compared to that obtained with molybdenum to tungsten-based metallizing (Figure 34) suggest a ternary effect between nickel, molybdenum and tungsten.

c. Flow brazing

The most significant test results obtained with flow-brazed seals are listed in Table 14. The Roman numeral in the

TABLE 14

Significant Test Results

Test	Atmosphere	Temperature (°C)	Hours	Significant Results (See Key)
45	Vacuum	1500	306	10 CNM, 10 TNM, 10 MNM - remained leak tight
49	Cesium	1500	306	14 CNA - Mo - remained leak tight
51	Cesium	1250	500	25 TNM - remained leak tight
52	Cesium	1250	500	26 TNM - remained leak tight
53	Cesium	1250	500	13 TNA, 17 TNA - Mo - remained leak tight
57	Cesium	1500	250	18 TNA - Mo - remained leak tight
60	Vacuum	1500	250	22 TNA - Mo - remained leak tight
64	Cesium	1500	250	35 CNA - Mo - remained leak tight, niobium alloy Cb 753 showed no attack
65	Vacuum	1250	855	No. 36 and 73 metallizings on A-976 showed no change
66	Vacuum	1250	855	Same as test 65
69	Vacuum	1500	230	5AIIIWIIIA-W, 7AIIIMIIIA-W, 4AVWVA-W - remained well bonded but ceramics cracked
73	Cesium	1500	230	9ANWNA-W - remained well bonded but ceramics cracked
83	Vacuum	1500	230	15AVMVA-W - remained well bonded but ceramics cracked
84	Vacuum	1500	230	No. 60 & 155 metallizing on A-976 and Lucalox alumina ceramics showed no significant change
85	Cesium	1500	230	Same as test 84
86	Cesium	1500	230	61ANMNA-W - remained in tact, but ceramics cracked
87	Cesium	1200	500	6AVIICVIIA - Bare, 6AVIITVIIA - Bare, 13AVMVA-W, 39ANMNA-W, 51ANMNA-W, 53ANMNA-W, 57ANMNA-W, and 73ANMNA-W - all remained leak tight
88	Vacuum	1200	500	5AVIICVIIA - Bare, 5AVIITVIIA - Bare, 12AVMVA-W, 45ANMNA-W, 46ANMNA-W, 56ANMNA-W, 58ANMNA-W and 72ANMNA-W all remained leak tight
89	Vacuum	1500	400	8AVIICVIIA - Bare - remained leak tight
90	Vacuum	1500	400	10AVIICVIIA - Bare - remained leak tight, 90 Ta - 8 W - 2 Hf alloy showed no loss of ductility cermet nickel braze-diffusion bonded to Mo - remained well bonded
92	Vacuum	1200	686	30 CNA - Mo, well bonded, 52ANMNA-W and 11AVMVA-W remained leak tight, 4AIIIWIIIA-W - remained well bonded
93	Cesium	1200	300	16AVMVA-W, 7AVIICVIIA - Bare, remained leak tight, 6AVWVA-W, 21AVMVA-W, previously sectioned, remained well bonded
94	Vacuum	1200	300	18AVMVA-W remained leak tight, 12AVMVA-W, 5AVIICVIIA - Bare, 5AVIITVIIA - Bare, 45ANMNA-W, 46ANMNA-W, 56ANMNA-W and 72ANMNA-W from test 88 remained leak tight
95	Vacuum	1500	255	5CVIIM, 5TVIIM, 9AVIICVIIA - Bare, remained leak tight
96	Vacuum	1500	255	28TNM, 25MNM, 9AVIITVIIA-W, 12AVIICVIIA-W, remained leak tight, 9AVIIMVIIA-W, remained bonded but ceramics cracked
97	Vacuum	1250	327	51ANMNA-W, 73ANMNA-W, 11AVMVA-W, 6AVIICVIIA, remained leak tight, three graded cermets remained leak tight
98	Vacuum	1250	327	56ANMNA-W, 72ANMNA-W, 12AVMVA-W, 10AVIITVIIA-W, 10AVIIMVIIA-W, remained leak tight, two graded cermets remained leak tight

Key: CNM = Niobium (columbium) nickel braze-diffusion-bonded to molybdenum ring
TNM = Tantalum nickel braze-diffusion-bonded to molybdenum ring
CNA - Mo = Niobium nickel braze-diffusion-bonded to molybdenum metallized alumina ceramic
AIIWIIIA-W = Tungsten (III) brazed between tungsten metallized alumina ceramics

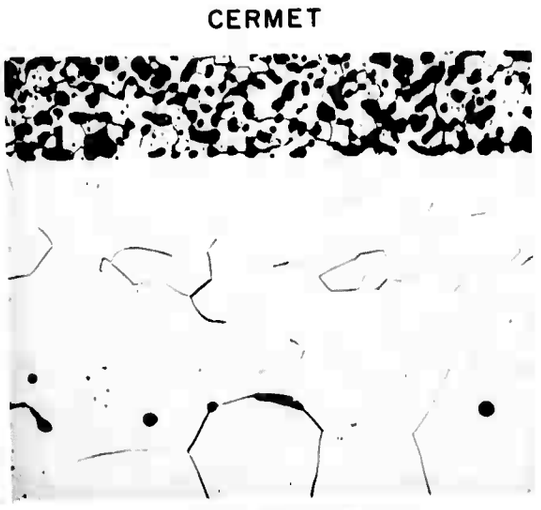

FIGURE 35 Molybdenum-Alumina Cermet Braze-Diffusion-Bonded to Molybdenum, After Test (250X)

specimen designations signifies which flow braze was used. The other letters are the same as explained under nickel braze-diffusion-bonding.

Braze III (38 w/o Cr - 62 w/o Pd) acted somewhat similar to nickel braze-diffusion-bonding when testing molybdenum brazed to tungsten-based metallizing at 1500°C. Figure 36 shows the pores that were formed from what appears to have been the presence of a liquid phase. Pores also formed at 1500°C with tungsten brazed to tungsten-based metallizing, which is also shown in Figure 36. However, in this case, the pores undesirably segregated to the tungsten-metallizing interface. At 1200°C, essentially no change occurs in either bond combination as is illustrated in Figure 36. Since no low melting phases are anticipated between chromium or palladium and tungsten or molybdenum, it may be possible to inhibit the formation of pores by a proper pretest diffusion treatment.

With braze V (50 w/o Nb - 30 w/o Pd - 20 w/o Ni) pore formation also occurred with molybdenum and tungsten brazed to tungsten-based metallizing, when testing at 1500°C as shown in Figure 37. Although these examples show most of the pores well within the metal members, others had the pores segregated to the metal-metallizing interface. As with nickel diffusion-bonding and with other brazes the metallizing became quite densified at the 1500°C test temperature. Testing at 1200°C caused no preceivable change in the bond structure, as is also illustrated in Figure 37.

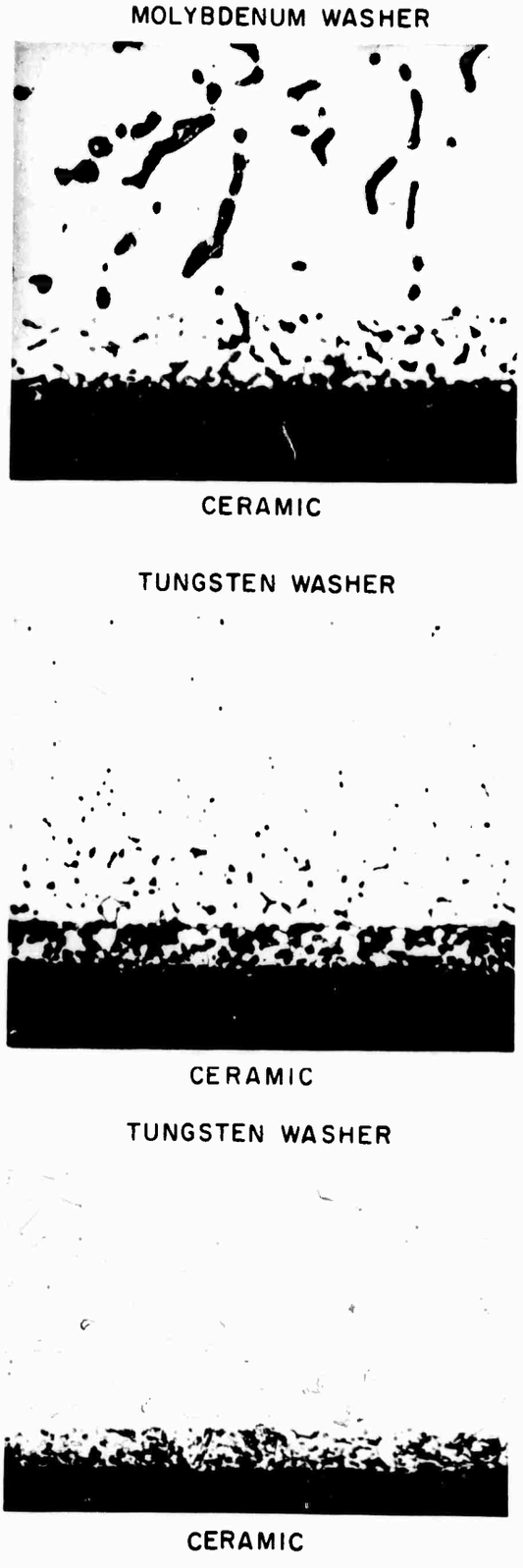

7A III M III A
NO. 73 METALLIZING
TESTED: 1500°C
230 HRS., VAC

5A III W III A
NO. 73 METALLIZING
TESTED: 1500°C
230 HRS., VAC

4A III W III A
NO. 73 METALLIZING
TESTED: 1200°C
686 HRS., VAC

FIGURE 36 Molybdenum and Tungsten Bonded with Braze III to Metallized Alumina Ceramics, After Test (250X)

MOLYBDENUM WASHER

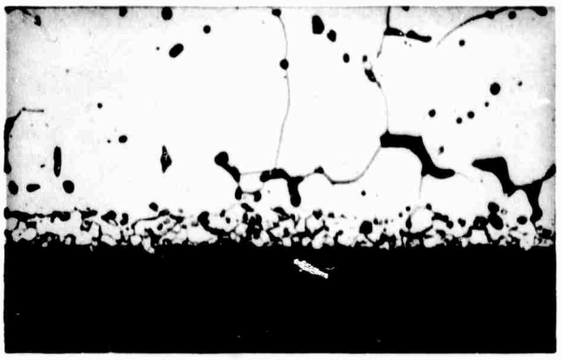

15 A V M V A
NO.155 METALLIZING
TESTED: 1500°C
230 HRS, VAC

CERAMIC

TUNGSTEN WASHER

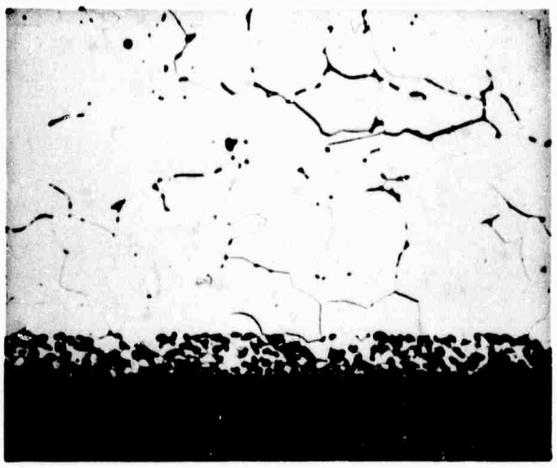

4 A V W V A
NO. 73 METALLIZING
TESTED: 1500°C
230 HRS, VAC

CERAMIC

MOLYBDENUM WASHER

21 A V M V A
NO.155 METALLIZING
TESTED: 1200°C
300 HRS, Cs

CERAMIC

FIGURE 37 Molybdenum and Tungsten Bonded with Braze V to Metallized Alumina Ceramics, After Test (250X)

Braze VII (67 w/o Nb - 33 w/o Fe), as previously mentioned, was found capable of producing leak-tight joints between the various structural metals and bare ceramics and, therefore, most of the ceramic seals made with braze VII were made in this manner. Figure 38 shows such a bond to niobium after testing at 1500°C. Although this bond is leak tight, it is very weak from apparent lack of mechanical interlocking. Similar bonds were obtained with tantalum, which remained leak tight through 1200°C testing, and molybdenum, but the bond formed with molybdenum, although leak tight initially, did not survive 1200°C testing. When brazing to tungsten-based metallizing, the niobium, tantalum, molybdenum bonds developed a few pores from 1500°C testing and considerable densification of the metallizing was present. The tantalum to tungsten-based metallizing braze specimen (9AVIITVIIA-W) had an "as tested" appearance very similar to specimen 31ANTNA-W shown in Figure 33. Seals consisting of niobium, tantalum and molybdenum discs brazed with braze VII to molybdenum rings were also tested at 1500°C and the effects on the bond structures are shown in Figure 38. Note the complete absence of any interface braze layer and the freedom from porosity. The very limited reaction with molybdenum in each case suggests that this braze may be well suited for brazing to molybdenum-based metallizing.

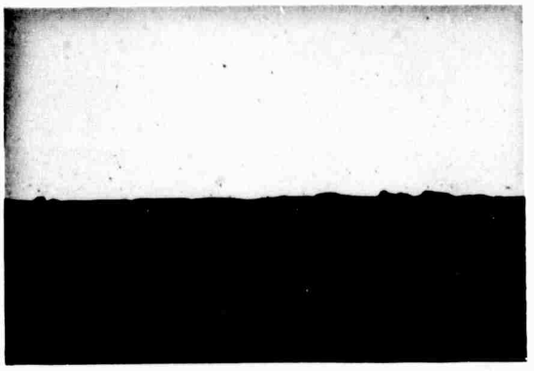

8 A VII C VII A
NO METALLIZING
TESTED: 1500°C
400 HRS., VAC

CERAMIC
NIOBIUM DISC

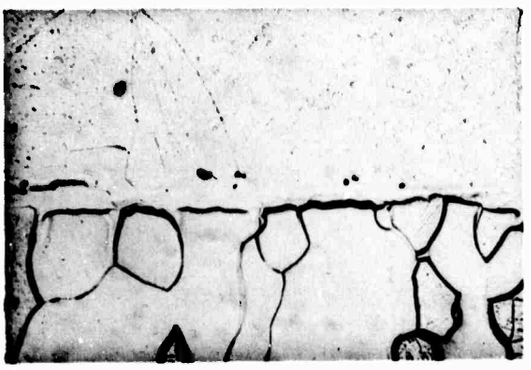

5 C VII M
TESTED: 1500°C
255 HRS., VAC

MOLYBDENUM RING
TANTALUM DISC

5T VII M
TESTED: 1500°C
255 HRS., VAC

MOLYBDENUM RING
MOLYBDENUM DISC

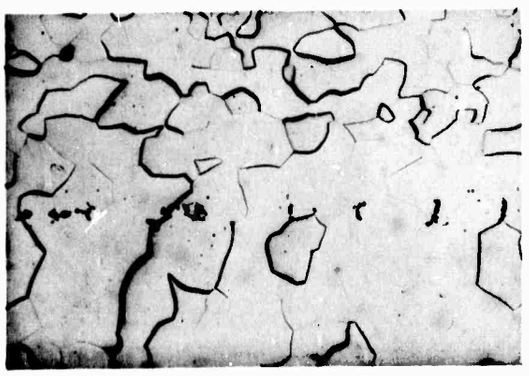

5 M VII M
TESTED: 1500°C
255 HRS., VAC

MOLYBDENUM RING

FIGURE 38 Bonds Made with Braze VII After Test (250X)

d. Materials

All of the materials tested showed negligible degradation from exposure to 20-Torr cesium or vacuum at 1500°C. The formation of apparent oxide phases in niobium and tantalum was previously discussed.(2) However, later tests indicate that by properly protecting the specimens, such as by wrapping in molybdenum and tantalum foil, the formation of these phases can be prevented. This was illustrated by the cleanliness of the niobium and tantalum shown in Figure 38.

Niobium alloy, Cb-753 (5 w/o V - 1.25 w/o Zr - Bal Nb obtained from Union Carbide Stellite Co.) was tested at 1250°C in vacuum and at 1500°C in cesium and vacuum. The "as tested" microstructures along with the "as received" microstructure are shown in Figure 39. There appears to have been some precipitation of a second phase from testing at 1250°C and 1500°C and also some grain growth at 1500°C. Since these temperatures are closer to the solutioning temperatures than the precipitation temperatures for this alloy and since these specimens were not well protected, the precipitate may be an oxide. Tantalum alloy, 90 w/o Ta - 10 w/o W (obtained from National Research Corp.), was tested in vacuum at 1250°C and showed no significant change in microstructure. A modification of this alloy, 90 w/o Ta - 8 w/o W - 2 w/o Hf (also obtained from NRC), was tested at 1500°C in vacuum, which resulted in considerable precipitate forming within the material as shown in Figure 40. The specimen was quite ductile after testing.

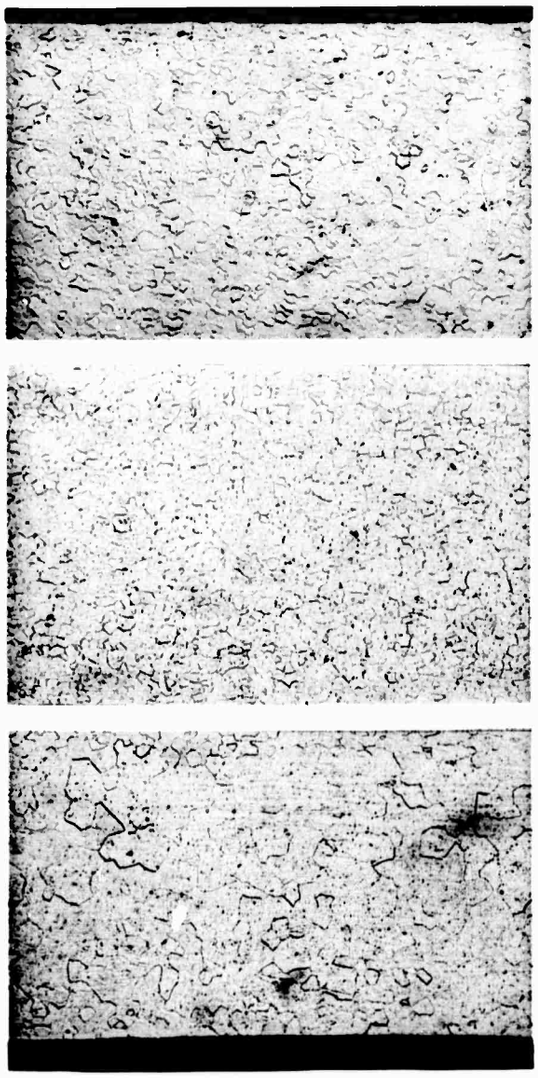

FIGURE 39 Niobium Alloy, Cb 753, Before and After Testing (100X)

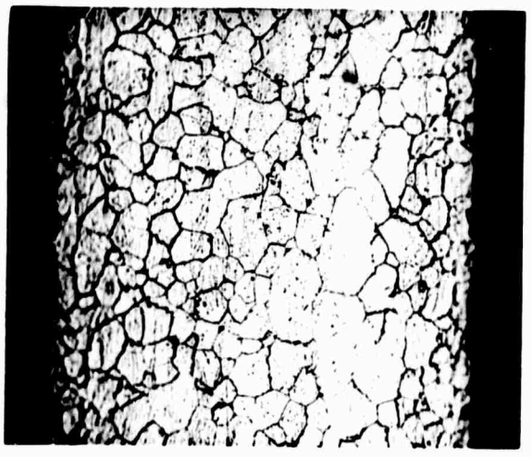

90 TA - 8 W - 2 Hf
AS RECEIVED

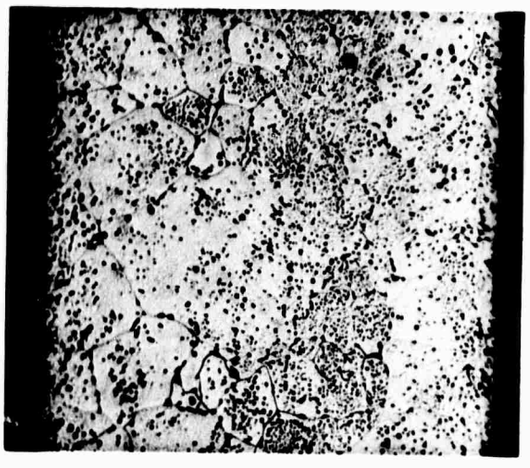

90 TA - 8 W - 2 Hf
TESTED: 1500°C
400 HRS., VAC

FIGURE 40 Tantalum Alloy, 90 Ta - 8 W - 2 Hf, Before and After Testing (250X)

Metallizing coating No. 36 (molybdenum) and No. 73 (tungsten) applied to A-976 alumina ceramic were tested at 1250°C in both vacuum and 20-Torr cesium. No changes over the metallized structures were noticed. Also tested in vacuum and 20-Torr cesium, but at 1500°C, were metallizing coatings No. 60 (tungsten) and No. 155 (tungsten) applied to both A-976 and Lucalox alumina ceramics. To assess the effect of evaporation, the specimens were stacked in pairs with a tungsten washer placed over the metallized coating of the bottom specimen. In vacuum, the weight loss from the top (metallizing exposed) specimens ranged from 5 to 10 times that of the bottom specimen, whereas in cesium the weight loss of the top specimen was about half that from vacuum but the bottom specimens lost almost the same amount. Assuming all of the weight loss was from the metallizing, the weight losses in cesium would be less than 5 percent. The effect of the atmosphere and 1500°C testing temperature is discussed under sub-task C-1.

Conclusions

1. Niobium to molybdenum or to molybdenum-based metallizing bonds, formed by nickel braze-diffusion-bonding, have useful service temperatures approaching 1500°C.

2. Tantalum to molybdenum, or to molybdenum- or tungsten-based metallizing bonds, formed by nickel braze-diffusion-bonding, have useful service temperatures to at least 1500°C.

3. Molybdenum to molybdenum-based metallizing bonds formed by nickel braze-diffusion-bonding have useful service temperatures to at least 1500°C. Molybdenum to tungsten-based metallizing bonds formed the same way, have a limited service temperature in the range of 1200 to 1500°C.

4. Tungsten to tungsten-based metallizing bonds formed by nickel braze-diffusion-bonding have useful service temperatures to at least 1500°C. The large thermal expansion mismatch between tungsten and alumina ceramic make it difficult to obtain leak-tight seals due to cracking of the ceramics.

5. Nickel braze-diffusion-bonding is a useful technique for sealing molybdenum-alumina cermets to molybdenum. The bond so formed has useful service temperatures to at least 1500°C.

6. Braze III (38 w/o Cr - 62 w/o Pd) bonds between molybdenum or tungsten and tungsten-based metallizing have a useful service temperature limit in the range of 1200 to 1500°C.

7. Braze V (50 w/o Nb - 30 w/o Pd - 20 w/o Ni) bonds between molybdenum or tungsten and tungsten-based metallizing have a useful service temperature limit in the range of 1200 to 1500°C.

8. Braze VII (67 w/o Nb - 33 w/o Fe) can be used to provide, between bare alumina ceramic and niobium, bonds which will remain leak tight through 1500°C exposure.

9. Niobium, tantalum and molybdenum to tungsten-based metallizing bonds formed by braze VII have useful service temperature approaching 1500°C.

10. Braze VII bonds between niobium, tantalum, or molybdenum and molybdenum improve with time and have useful service temperatures in excess of 1500°C.

11. The materials niobium, niobium alloy Cb-753, tantalum, 90 w/o Ta - 8 w/o W - 2 w/o Hf, molybdenum and tungsten show no apparent degradation in vacuum or cesium vapor, if sufficiently free of oxygen, up to at least 1500°C.

References

1. GEST-2035, "Final Technical Summary Report of Research and Development Program of Thermionic Conversion of Heat to Electricity", Volume I, June 30, 1964, NObs-88578.

2. GEST-2046 "Technical Summary Report of Research and Development Program of Thermionic Conversion of Heat to Electricity", December 31, 1964, NObs-90496.

3. "Research and Development Program on Thermionic Conversion of Heat to Electricity", Quarterly Progress Report No. 3, March 31, 1965.